Detonability Study of Liquid Hydrazine

Benjamin O. Garcia
David J. Chavez
Lockheed
White Sands Test Facility
Las Cruces, New Mexico

Larry J. Linley
NASA
White Sands Test Facility
Las Cruces, New Mexico

ABSTRACT

This paper presents the results of a study conducted at NASA White Sands Test Facility (WSTF) on the shock detonability of liquid hydrazine. Liquid hydrazine is the propellant used in the propulsion modules for Space Station Freedom. The focus of this study was to investigate the shock sensitivity of liquid hydrazine subjected to a hypervelocity projectile impact. This study provides the minimum power density needed for the initiation of homogenous liquid hydrazine, and thus provides the information needed to conduct a meaningful impact test on liquid hydrazine's shock detonability.

BACKGROUND

WSTF, in the past, has performed tests that attempted to shock-initiate liquid hydrazine and found no evidence of hydrazine reaction (see references 1 and 2). The most recent test on the shock detonability of liquid hydrazine was conducted by Science Applications International Corporation (SAIC) for Eglin Air Force Base (see reference 3). The SAIC test suggested that there was some evidence of hydrazine reaction, although the details of their results were poorly substantiated. The following is a short synopsis of the previous tests:

1) Condensed Phase Detonation Studies, WSTF # 90-24354, dated September 28, 1990. 887 g of C-4 was detonated on top of a stainless steel tube (4 in. x 10 in. long) filled with liquid hydrazine. The liquid hydrazine did not detonate or sustain a reaction.

2) Demonstration of Hazardous Hypervelocity Test Capability, TR-692-00l, dated September 24, 1991. A 1/8-in. aluminum projectile was shot with a velocity of 6.1 km/sec at a 300-ml stainless steel vessel filled with liquid hydrazine. The liquid hydrazine did not detonate or sustain a reaction.

3) Fuel Tank Explosion Lethality, SAIC 91-5425-SH, dated April 1991. A 100-g cylindrical projectile was shot with a velocity of 5.0 km/sec at an aluminum, 100-mm-diameter spherical

Report Documentation Page

Form Approved
OMB No. 0704-0188

Public reporting burden for the collection of information is estimated to average 1 hour per response, including the time for reviewing instructions, searching existing data sources, gathering and maintaining the data needed, and completing and reviewing the collection of information. Send comments regarding this burden estimate or any other aspect of this collection of information, including suggestions for reducing this burden, to Washington Headquarters Services, Directorate for Information Operations and Reports, 1215 Jefferson Davis Highway, Suite 1204, Arlington VA 22202-4302. Respondents should be aware that notwithstanding any other provision of law, no person shall be subject to a penalty for failing to comply with a collection of information if it does not display a currently valid OMB control number.

1. REPORT DATE	2. REPORT TYPE	3. DATES COVERED
AUG 1994		**00-00-1994 to 00-00-1994**

4. TITLE AND SUBTITLE	5a. CONTRACT NUMBER
Detonability Study of Liquid Hydrazine	5b. GRANT NUMBER
	5c. PROGRAM ELEMENT NUMBER
6. AUTHOR(S)	5d. PROJECT NUMBER
	5e. TASK NUMBER
	5f. WORK UNIT NUMBER
7. PERFORMING ORGANIZATION NAME(S) AND ADDRESS(ES) **Lockheed,White Sands Test Facility, ,Las Cruces,NM,88004**	8. PERFORMING ORGANIZATION REPORT NUMBER
9. SPONSORING/MONITORING AGENCY NAME(S) AND ADDRESS(ES)	10. SPONSOR/MONITOR'S ACRONYM(S)
	11. SPONSOR/MONITOR'S REPORT NUMBER(S)

12. DISTRIBUTION/AVAILABILITY STATEMENT
Approved for public release; distribution unlimited

13. SUPPLEMENTARY NOTES
See also ADM000767. Proceedings of the Twenty-Sixth DoD Explosives Safety Seminar Held in Miami, FL on 16-18 August 1994.

14. ABSTRACT
see report

15. SUBJECT TERMS

16. SECURITY CLASSIFICATION OF:			17. LIMITATION OF ABSTRACT	18. NUMBER OF PAGES	19a. NAME OF RESPONSIBLE PERSON
a. REPORT **unclassified**	b. ABSTRACT **unclassified**	c. THIS PAGE **unclassified**	**Same as Report (SAR)**	**46**	

vessel filled with liquid hydrazine. The test results indicated that some reaction of liquid hydrazine occurred, although not enough evidence was gathered to emphatically verify that a detonation occurred.

Given the differences in these results, this study was conducted in an attempt to investigate in detail the shock stimuli that would be necessary to achieve an appreciable hydrazine reaction. The methodology employed was one used by C. L. Mader in his success with modeling homogeneous energetic materials using Arrhenius kinetic parameters determined from laboratory thermal stability experiments. Mader was very successful at numerically reproducing the shock initiation of nitromethane observed in experiment.

PURPOSE

An energetic material is one which decomposes exothermically, i.e., with the release of heat. By this definition liquid hydrazine, a monopropellant, is an energetic material and therefore should detonate given the proper shock stimuli. This study investigates fundamental information on the appropriate stimulus needed to achieve a detonation. Specifically, this study provides the minimum power density needed for the detonation of homogenous liquid hydrazine. The term power density implies the pressure and time duration sustained by a projectile in order to provide sufficient heat for attaining the critical temperature for a detonable condition. The result of this study is a proposed experiment aimed at reproducing the most realistic situation in which a hypervelocity projectile impact might initiate homogenous liquid hydrazine.

APPROACH

The initial effort of this study was to investigate, in detail, previous tests conducted by others. Hydrodynamic models of each experiment were calculated to determine the pressure and duration delivered to the liquid hydrazine. Then, as chemical kinetic parameters were determined, reactive hydrodynamic models were constructed to determine if the results of the experiments could be duplicated. If successful, a numerical model would be formulated to design an experiment that would replicate actual conditions that might exist for a titanium tank filled with liquid hydrazine on board Space Station Freedom.

The previous tests were modeled using the hydrocodes SIN, TDL, and ZEUS. The employment of these codes is shown in the flow diagram below. The following list expands on the approach as summarized in the flow diagram.

1. Determine the unreacted equation of state (EOS) of liquid hydrazine.

For accurately determining the variables of other shock states, the EOS of any substance is usually required, being the equation that bridges the gap with mass, momentum, and energy. This is an experimental plane in which the shock velocity and particle velocity (or free surface velocity) are measured. The proposed method for determining the EOS was one used by McQueen and Rice of Los Alamos National Laboratory. The test method uses an impedance

matching technique in which a projectile with a known EOS impacts a target with an unknown EOS at a fixed impact velocity. By measuring the shock velocity and knowing the initial density of the known material, one can determine the Rayleigh line, that will intersect the projectile shock hugoniot at one point. By repeating the procedure for different impact velocities and determining the different slopes of the Rayleigh line, one can construct the shock hugoniot of the unknown material. A minimum of six shots at different velocities are needed to determine the EOS.

One alternative to the above method was to make some assumptions about homogenous hydrazine and input these parameters into a code called SEQS (Solid Equation of State). This code will generate single shock hugoniots in the temperature vs specific volume plane, pressure vs particle velocity plane, and shock velocity vs particle velocity plane. The results of these computations are shown in Appendix A.

2. Determine the reactive hugoniot equation of state for the detonation products.

A description of the expansion isentrope for the detonation products is needed to determine the C-J pressure and velocity. The code used to determine this information was the BKW (BeckerKistiakowski-Wilson) code. This code performs a chemical equilibrium balance and generates an expansion isentrope, a curve for the reaction products in the pressure vs specific volume plane. The results of this computation are shown in Appendix B.

3. Perform thermal stability experiments.

Thermal stability experiments are needed to determine the chemical reaction rate, products, critical temperatures, and activation energy for liquid hydrazine. These quantities are constants for the Arrhenius rate law for burn, which is needed to perform hydrodynamic calculations in the SIN and TDL codes. The information for this section was taken from tests performed by the New Mexico Institute of Mining and Technology (NMT) in Socorro, New Mexico. Their results are shown in Appendix C.

4. Determine the minimum power density for steady-state detonation.

One-dimensional hydrocode calculations were performed using SIN. This code is used to model explosive flow using one-dimensional Lagrangian, reactive hydrodynamics. The SIN code was the primary workhorse for modeling the previously conducted tests and in determining the detonability of liquid hydrazine for the proposed experiment. After determining the conditions (i.e. the power density requirement) for attaining a steady-state detonation, a two-dimensional Lagrangian, reactive hydrocode calculation was performed to determine the effects of geometry on the release wave attenuation. The code used to perform these calculations was TDL. The two-dimensional calculations were augmented by calculations using the Zeus code. This code provided a check on the shock pressures generated in the liquid hydrazine. The results of these calculations are presented in the results section.

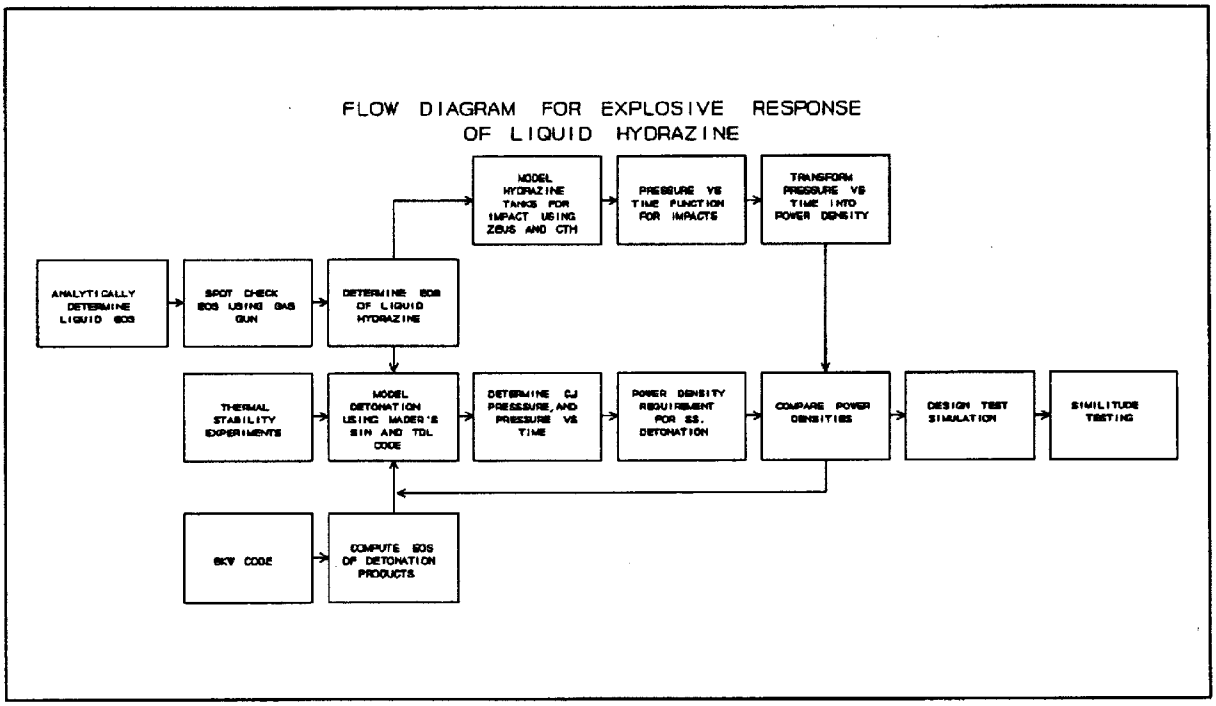

Flow Diagram for Explosion Response of Liquid Hydrazine

RESULTS

The tests performed by other investigators were numerically modeled with the following assumptions. A shock travels into the homogenous hydrazine, compressing and heating the propellant. The shock heating results in chemical decomposition that accelerates exponentially. The reaction begins at the rear boundary, because it has been hot the longest, and a detonation wave propagates at the C-J state of the shock propellant. This type of bulk heating or thermal initiation analysis has been successfully performed by C. L. Mader for homogenous energetic materials using the Frank-Kamenetskii equation with the Arrhenius chemical kinetics. Using this type of analysis, each test was modeled to investigate the shock stimuli provided in each situation and to formulate the minimum power density that would be required for steady-state detonation.

Condensed Phase Detonation Studies

This test was modeled using the SIN code with the chemical kinetic parameters provided by NMT. The result of this calculation indicated that the shock wave generated by the C-4 explosive was not sufficient to generate a hydrazine reaction. The shock pressure into the hydrazine was 150 kbar with a duration of approximately 2 microseconds. Figure l in Appendix D shows the shock pressure generated into the liquid hydrazine and Figure 2 shows that no reaction occurred.

Demonstration of Hazardous Hvpervelocity Test Capability

This test was modeled using the TDL code with the same chemical kinetics as above and the Zeus code with no chemical kinetics. Zeus calculations were performed to provide a better representation of the shock wave generated by the sphere impacting the cylindrical vessel. This model shows that the release waves attenuate the shock wave into the liquid hydrazine very quickly, thus rendering an ineffective shock wave in the hydrazine. The pressure and duration, as calculated by Zeus, were 83 kbar and approximately .8 microseconds, which is in agreement with the TDL calculations. Figure 3 shows the shock pressure generated into the liquid hydrazine. The results of the TDL code calculation revealed that the pressure generated by the aluminum projectile was not sufficient to generate a hydrazine reaction. Figure 4 shows the initial projectile impact and Figure 5 shows that no hydrazine reaction occurred.

Fuel Tank Explosion Lethality

This test was modeled using the SIN code with the same chemical kinetics as above and the Zeus code with no chemical kinetics. The results of the SIN code calculation revealed that the shock wave generated by the aluminum projectile was sufficient to attain some decomposition of hydrazine. One reason a higher shock pressure was generated into the liquid hydrazine as compared to the other experiments was the impedance matching of materials adjacent to the liquid hydrazine. Figures 6 and 7 represent a pictorial view of the shock impedance matching of the SAIC test and the Condensed Phase Detonation Study. The pressure and duration as calculated by SIN was 285 kbar and approximately 5 microseconds. Figure 8 shows the

shock pressure generated into the liquid hydrazine and Figure 9 shows the amount of decomposition. The pressure and duration as calculated by Zeus was 267 kbar and approximately 1.5 microseconds, which is in agreement with the SIN calculations. Figure 10 shows the shock pressure generated into the liquid hydrazine. Another reason there was more hydrazine decomposition in this test as compared to the other tests was that the projectile geometry sustained the shock pressure for a longer duration before the release wave reduced its magnitude.

Proposed Experiment

The goal of this study was to use the information gathered from analyzing the previous tests to formulate a test situation in which the minimum power density requirement was met, replicating the actual hydrazine tank conditions existing on board Space Station Freedom. This experiment was created from a numerical model which simulated a steel slug impacting a titanium vessel filled with liquid hydrazine. The projectile was designed to be a cylinder to provide the sustained pressure necessary to generate enough shock heating. This experiment was also designed such that the projectile velocities could be achieved with WSTF's 1-in. light gas gun. The desired projectile velocity was between 7-7.5 km/sec. This experiment was modeled using SIN and TDL with the same chemical kinetics as above and the Zeus code with no chemical kinetics. The result of the SIN and TDL model revealed that the shock wave generated by the steel slug was sufficient to achieve a substantial amount of hydrazine reaction. The shock pressure into the hydrazine, as calculated by SIN, was 600 kbar with a duration of approximately 2.4 microseconds. Figure 11 shows the shock pressure generated into the liquid hydrazine and Figure 12 shows the amount of decomposition. Figure 13 shows the amount of hydrazine decomposition as calculated by TDL.

The pressure and duration, as calculated by Zeus, was 600 and approximately 1 microsecond, which is in agreement with the TDL calculations. Figure 14 shows the shock pressure generated into the liquid hydrazine.

Table 1 is presented as a comparison of the results for all tests and the proposed experiment. The relative ranking is based on the power density requirement for homogenous materials, which is

EQUATION

$$P^2\tau$$

This implies the pressure, P applied for a stock duration of τ.

CONCLUSIONS

Numerical reactive models of the WSTF tests and the SAIC test successfully reproduced their respective test results. The WSTF tests and the SAIC test emphasized that under particular shock loading conditions a minimum power density is required to achieve a hydrazine reaction. These models suggest that there is increased shock heating as a function of power density applied to the liquid hydrazine for each case. Analyzing previously conducted experiments provided a platform from which the proposed experiment has been suggested. This analysis has provided the most realistic power density required to achieve hydrazine reaction in a titanium tank. Future work should consider tests in which many parameters in reactive modeling are unknown for propellants. This should also include a program of determining the equations of state of propellants used by NASA and other agencies, and a program of enhancing a data base of kinetic parameters for various propellants specifically for inputs into reactive hydrodynamic models. Finally, the proposed experiment should be carried out to verify the results of the current modeling effort. This should not be looked at as a pass or fail experiment but only as a tool for verifying the suspected parameters which were calculated. This experiment needs to employ enough detailed instrumentation so that there would be sufficient information on the extent of the hydrazine reaction and to verify model parameters for future tests.

ACKNOWLEDGMENT

The authors are indebted to C. L. Mader of Mader Consulting Company, Honolulu, Hawaii, who spent many hours of his time in providing us with his knowledge in numerical modeling of explosives.

REFERENCES:

l. Rathgeber, K.; Radel, B. "Condensed Phase Detonation Studies." White Sands Test Facility special test data report WSTF # 90-24354, September 28, 1990.

2. Rucker, M. A.; Beeson, H.; Stoltzfus, J. M.; Benz, F. J. "Demonstration of Hazardous Hypervelocity Test Capability." White Sands Test Facility test report TR-692-001, September 24, 1991.

3. Wilson, C. W.; Warne, D.; Chatfield, M. D. "Fuel Tank Explosion Lethality." SAIC Technical Report SAIC 91-5425-SH, Shalimar, FL, April 1991.

4. Mader, C. L. "Numerical Modeling of Impact Involving Energetic Materials." In High Velocity Impact Dynamics by Jonas A. Zukas, 1990.

5. Mader, C. L. Numerical Modeling of Detonations. LANL, Los Alamos, 1979.

6. Axworthy, A. E.; Sullivan, J. M.; Cohz, S.; Welz, E. S. "Research on Hydrazine Decomposition." Final Report AFRPL-TR-69-146, Rocketdyne, Canoga Park, Calif., July

1969.

7. Bishop, C. V.; Miller, E. L.; Benz, F. J. "Liquid Propellant Thermal Hazard Estimation using Differential Scanning Calorimetry." In JANNAF Safety and Environmental Protection Subcommittee Meeting, 1983.

8. Schmidt, E. W. "Hydrazine and its Derivatives." Rocket Research Company, Redmond, Washington, Nov. 1983.

9. Wedlich, R. C.; Davis D. D. "Non-Isothermal Kinetics of Hydrazine Decomposition." Elsevier Science Publishers
B. V. Amsterdam, January 1990.

10. Audrieth, L. F.; Ackerson, B. The Chemistry of Hydrazine. University of Illinois, January 1951.

11. Benz, F. J. ; Bishop, C. V.; Pedley, M. D. "Ignition and Thermal Hazards of Selected Aerospace Fluids." RD-WSTF-0001 White Sands Test Facility, October 1988.

12. Thadhani, N. Class notes from "Dynamic Deformation of Solids." New Mexico Institute of Mining and Technology, January 1992.

13. Walker, F. E. "Discussion on Shock Initiation and P^2T," in Proceedings of the Sixth Symposium (International) on Detonation, pp. 82-85, ACR-221, U.S. Gov. Printing Office, Washington, D.C., 1976.

14. de Longueville, Y.; Fauquignon, C.; Moulard, H.; "Initiation of Several Condensed Explosives by a Given Duration Shock Wave," in Proceedings of the Sixth Symposium (International) on Detonation, pp. 105-114, ACR-221, U.S. Gov. Printing Office, Washington, D.C., 1976.

APPENDIX A
Solid Equation of State

Solid Equation of State Calculation for ** Hydrazine

Us = 1.5000OOE-01 + 1.500000E+00 Up from po to 1.050000E+00 megabars

The Initial Density is 1.00000000000E+00 g/cm^3

The Compressibility is 5. 00000000000E+0l

The Linear Coefficient of Expansion is 6. 00000000000E-05

The Initial Temperature is 3. 00000000000E+02

The Heat Capacity is 1. 00000000000E+00

The Volume Increlaent is 2. 00000000000E-04

The Temperature fit is between 1.000000E-04 and 5.000000E-01 megabars
ln(T)= 5.69480500000E+00 -3.62450400000E-0llnV -
1. 88700200000E+00lnV*2
-4.40056400000E+00lnV*3 1.74659500000E+00lnV*4

Vo!ume g/cm^3	Pressure	Temperature	K Shock	Particle
Velocity	mbars		Velocity	
1.000000E+00	0.000000E+00	3.E00000E+02	1.500000E-0T	0.000000E+00
9.980003E-01	4.526521E-05	3.000516E+02	1.504513E-01	3.008644E-04
9.960005E-01	9.107763E-05	3.001032E+02	1.509053E-01	6.035368E-04
9.940008E-01	1.374447E-04	3.001549E+02	1.513621E-01	9.080569E-04
9.920011E-01	1.843741E-04	3.002066E+02	1.518216E-01	1.214415E-03
9.900013E-01	2.318734E-04	3.002584E+02	1.522840E-01	1.522640E-03
9.880016E-01	2.799506E-04	3.003102E+02	1.527491E-01	1.832744E-03
9.860018E-01	3.286135E-04	3.003622E+02	1.532171E-01	2.144754E-03
9.840021E-01	3.778703E-04	3.004142E+02	l.536880E-01	2.458682E-03
9.820024E-01	4.277291E-04	3.004664E+02	1.541618E-01	2.774547E-03
9.800026E-01	4.781985E-04	3.005187E+02	1.546385E-01	3.092359E-03
9.780029E-01	5.292867E-04	3.005712E+02	1.551182E-01	3.412147E-03
9.760032E-0l	5.810026E-04	3.006238E+02	1.556009E-01	3.733933E-03
9.740034E-01	6.333549E-04	3.006766E+02	1.560866E-01	4.057715E-03
9.720037E-01	6.863524E-04	3.007297E+02	1.565753E-01	4.383534E-03

9.700040E-01	7.400044E-04	3.007830E+02	1.570671E-01	4.711390E-03
9.680042E-01	7.943200E-04	3.008365E+02	1.575620E-01	5.041321E-03
9.660045E-01	8.493086E-04	3.008903E+02	1.580600E-01	5.373329E-03
9.640048E-01	9.049798E-04	3.009443E+02	1.585612E-01	5.707453E-03
9.620050E-01	9.613432E-04	3.009987E+02	1.590655E-01	6.043693E-03
9.600053E-01	1.018409E-03	3.010534E+02	1.595731E-01	6.382078E-03
9.580055E-01	1.076187E-03	3.011085E+02	l.600840E-01	6.722639E-03
9.560058E-01	1.134687E-03	3.011639E+02	1.605981E-01	7.065386E-03
9.540061E-01	1.193920E-03	3.012197E+02	1.611155E-01	7.410338E-03
9.520063E-01	1.253896E-03	3.012759E+02	1.6l6363E-01	7.757515E-03
9.500066E-01	1.314627E-03	3.013326E+02	1.621604E-01	8.106947E-03
9.480069E-01	1.376122E-03	3.013898E+02	l.626880E-01	8.458654E-03
9.460071E-01	1.438394E-03	3.014474E+02	1.632190E-01	8.812666E-03
9.440074E-01	1.501453E-03	3.015056E+02	1.637535E-01	9.168983E-03
9.420077E-01	1.565311E-03	3.015642E+02	1.642915E-01	9.527643E-03
9.400079E-01	1.629980E-03	3.016235E+02	1.648330E-01	9.888679E-03
9.380082E-01	1.695472E-03	3.016834E+02	1.653781E-01	1.025209E-02
9.360085E-01	1. 761798E-03	3. 017439E+02	l. 659269E-01	1. 061792E-02
9.340087E-01	1.828971E-03	3.018051E+02	1.664793E-01	1.098618E-02
9.320090E-01	1.897005E-03	3.018669E+02	1.670354E-01	1.135690E-02
9.300092E-01	1.965910E-03	3.019294E+02	1.675952E-01	1.173011E-02
9.280095E-01	2.035701E-03	3.019928E+02	1.681588E-01	1.210583E-02
9.260098E-01	2.106391E-03	3.020569E+02	1.687261E-01	l.248408E-02
9.2401OOE-01	2.177994E-03	3.021218E+02	1.692974E-01	1.286490E-02
9.220103E-01	2.250522E-03	3.021875E+02	1.698725E-01	1.324830E-02
9.200106E-01	2.323990E-03	3.022542E+02	1.704515E-01	1.363431E-02
9.180108E-01	2.398412E-03	3.023217E+02	1.710345E-01	1.402298E-02
9.160111E-01	2.473803E-03	3.023903E+02	1.716215E-01	1.441430E-02
9.140114E-01	2.550177E-03	3.024598E+02	1.722125E-01	1.480832E-02
9.120116E-01	2.627550E-03	3.025304E+02	1.728076E-01	1.520506E-02
9.100119E-01	2.705936E-03	3.026021E+02	1.734068E-01	1.560456E-02
9.080122E-01	2.785352E-03	3.026748E+02	1.740102E-01	1.600683E-02
9.060124E-01	2.865813E-03	3.027487E+02	1.746179E-01	1.641191E-02
9.040127E-01	2.947336E-03	3.028239E+02	1.752298E-01	1.681983E-02
9.020129E-01	3.029936E-03	3.029002E+02	1.758460E-01	1.723063E-02
9.000132E-01	3.113631E-03	3.029779E+02	1.764665E-01	1.764432E-02

FIGURE 2

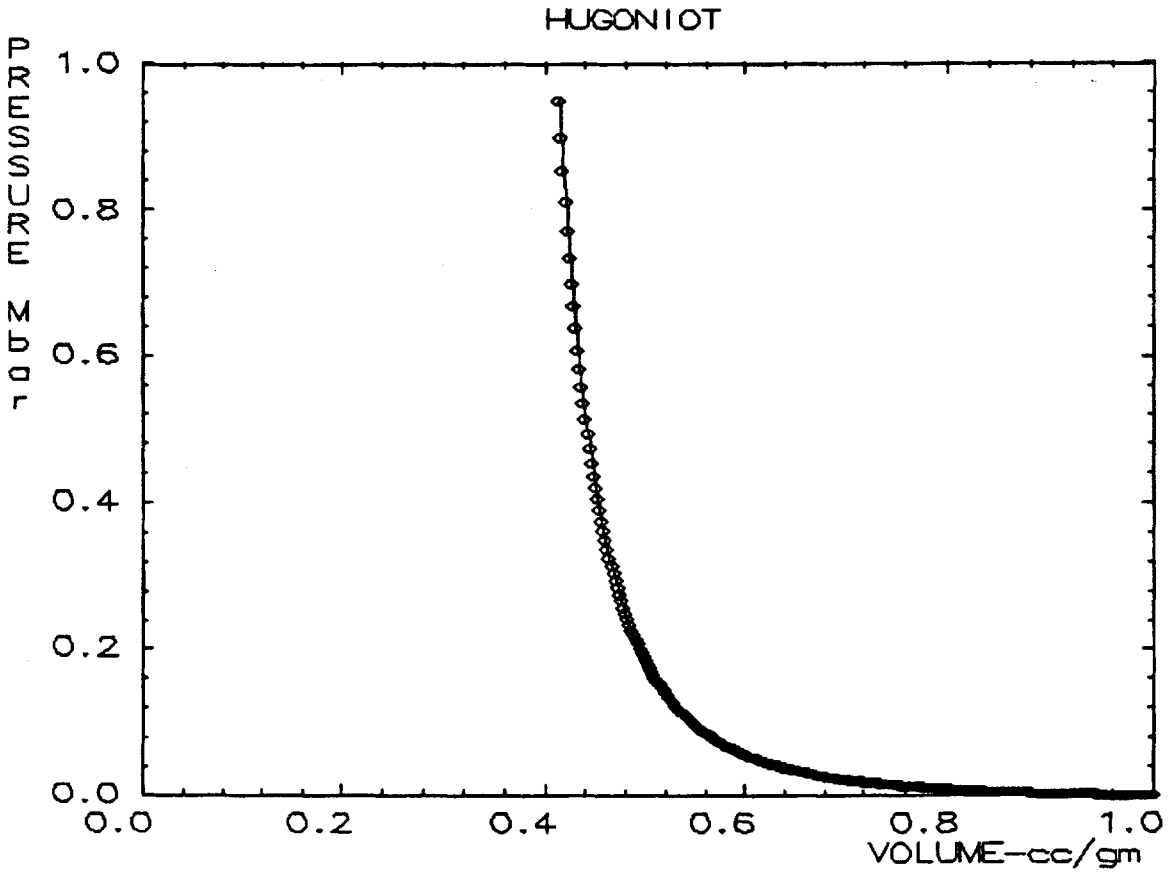
HUGONIOT
PRESSURE Mbar
1.0
0.8
0.6
0.4
0.2
0.0
0.0
0.2
0.4
0.6
0.8
1.0
VOLUME–cc/gm

FIGURE 3

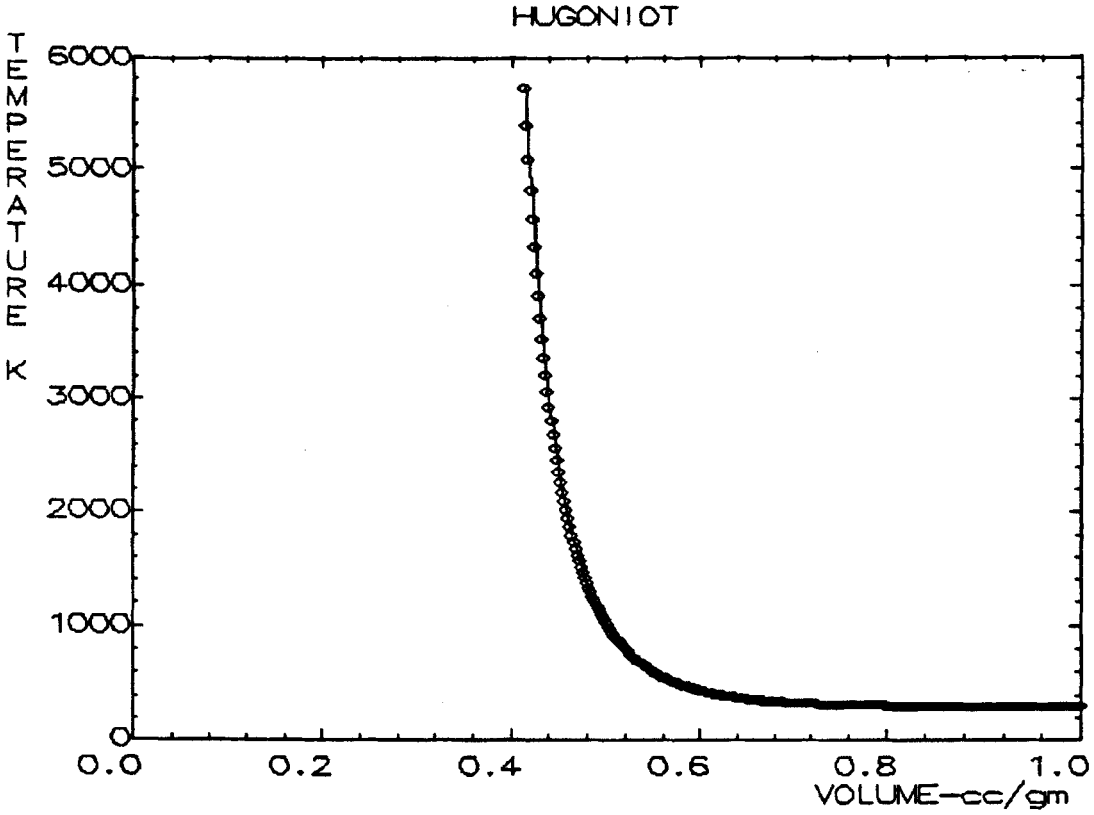
HUGONIOT
TEMPERATURE K
6000
5000
4000
3000
2000
1000
0
0.0
0.2
0.4
0.6
0.8
1.0
VOLUME—cc/gm

FIGURE 4

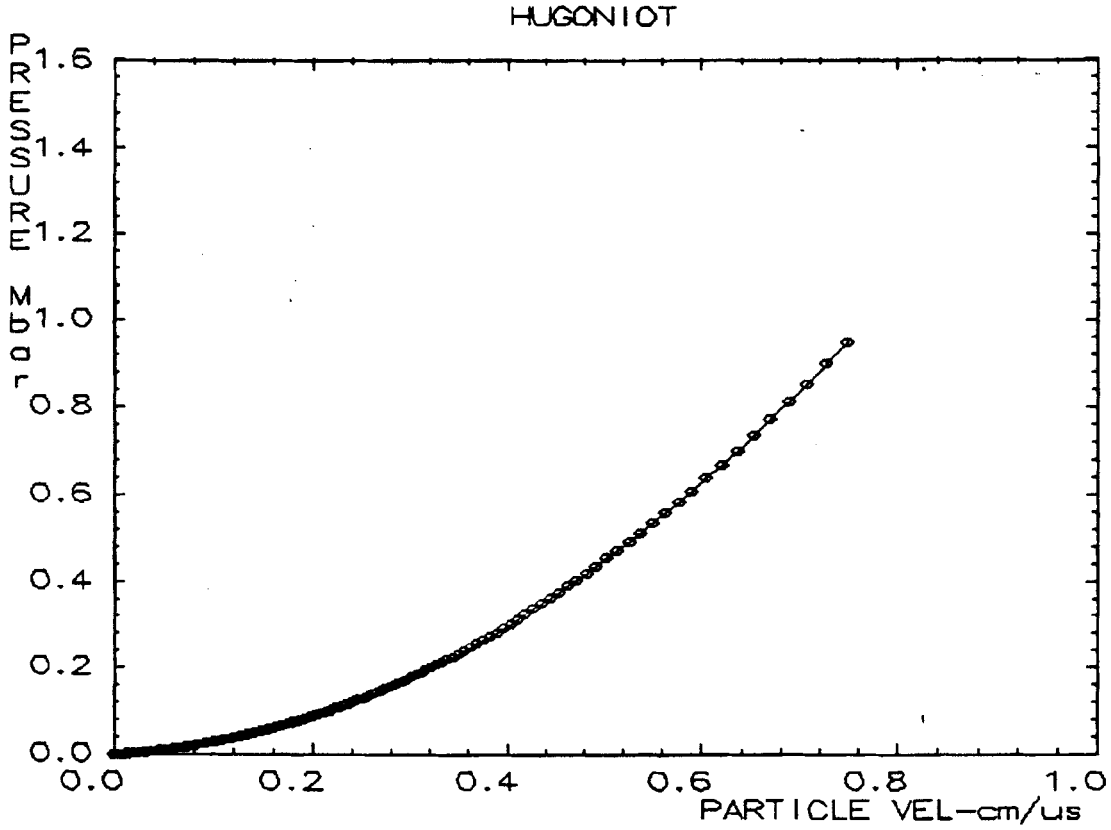
HUGONIOT
PRESSURE Mbar
1.6
1.4
1.2
1.0
0.8
0.6
0.4
0.2
0.0
0.0
0.2
0.4
0.6
0.8
1.0
PARTICLE VEL-cm/us

FIGURE 5

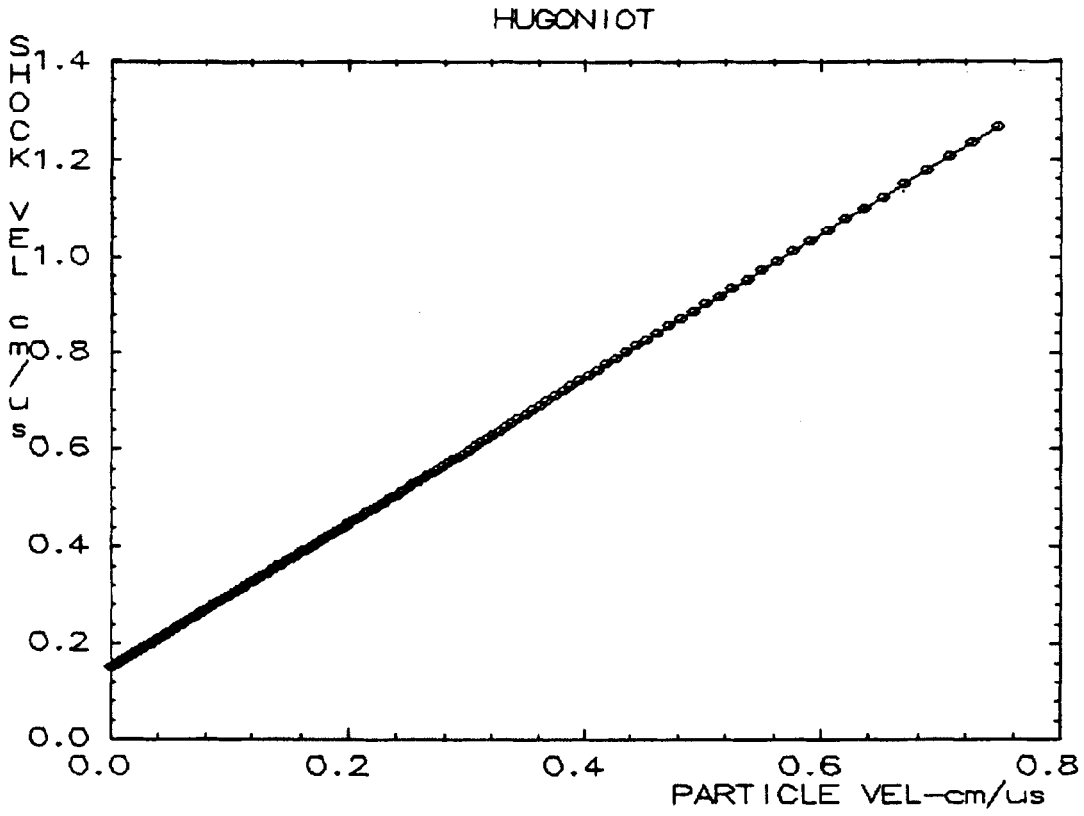
HUGONIOT
SHOCK VEL cm/us
1.4
1.2
1.0
0.8
0.6
0.4
0.2
0.0
0.0
0.2
0.4
0.6
0.8
PARTICLE VEL-cm/us

APPENDIX B
BKW Equation of State

constant	with	idenity	no	5	is	4.00000000000E+02
constant	with	idenity	no	5	is	4.00000000000E+02
constant	with	idenity	no	11	is	1.50000000000E-01
constant	with	idenity	no	11	is	1.50000000000E-01
constant	with	idenity	no	19	is	5.00000000000E-01
constant	with	idenity	no	19	is	5.00000000000E-01
constant	with	idenity	no	9	is	9.50000000000E-01
constant	with	idenity	no	9	is	9.50000000000E-01
constant	with	idenity	no	14	is	l.50000000000E-01
constant	with	idenity	no	14	is	1.50000000000E-01
constant	with	idenity	no	16	is	9.50000000000E-01
constant	with	idenity	no	16	is	9.50000000000E-01
constant	with	idenity	no	18	is	1.05000000000E+00
constant	with	idenity	no	18	is	1.05000000000E+00

A FORTRAN BKW Calculation for the Explosive Hydrazine for Garcia- Large NH3 Covolume

The Number of Elements is 2

The Number of Gas Species is 4

The Number of Solid Species is 0

The BKW Equation of State Parameters are
Alpha= 5.000000E,-01 Beta= 1.60000E-01 Theta= 4.00000E+02
Kappa= 1.0909780E+0l

The Composition of the Explosive is
2.0000000E+00 Moles of n
4.0000000E+00 Moles of h

The Density of the Explosive is 1.0110000E+00, g/cm^3

The Molecular Weight is 3.2045280E+0l grams

The Heat of Formation at 0 deg K is 1.0500000E+04 Calories per Formula Weight The Solid (Cowan)

Equation of State parameters V0, AS, BS, CS, DS, ES,

The Input Detonation Product Elemental Composition Matrix
.2E+0l OE+00 0E+00 .2E+0l lE+0l .3E+0l 0E+00
lE+0l

A FORTRAN BKW Calculation for the Explosive Hydrazine for Garcia- Large NH3 Covolume

The Computed CJ Pressure is 1.1229070E-01 megabars

The Computed Detonation Velocity is 7.5930330E-01 cm/microsecond

The Computed CJ Temperature is 3.4224570E+02 Degrees Kelvin

The Computed CJ Volume 7.9857050E-01 cc/gm of Explosive

The Computed Gamma is 4.1908430E+00

The Volume of the Gas is 8.53009E+00 cc/mole 3.00002E+00

Moles of Gas

Solid Volume in cc/cm

The C-J Composition of the Detonation Products and the Input Coef f icients

Specie	No of Moles	Coef f icients A,B,C,D,E,	the I C,	Heat For,	Covolume
n2	1.000004E+00	4.392340E+0l	1.222501E-02	-2.379005E-06	1.798322E-10
		0.000000E+00	1.139161E+03	0.000000E+00	3.800000E+02
h2	2.000012E+00	2.970347E+0l	1.143829E-02	-2.201222E-06	1.677761E-10
		O.000000E+00	1.175896E+03	0.000000E+00	8.000000E+0l
nh3	1.000000E-08	4.201816E+0l	1.911662E-02	-3.164330E-06	2.197801E-10
		0.000000E+00	1.206961E+03	-9.368000E+03	4.760000E+03
h	l.000000E-08	2.639110E+0l	8.121372E-03	-l.690740E-06	1.316823E-10
		0.00000E+00	7.946316E+02	5.161900E+04	7.600000E+0l

The BKW Hugoniot for the Detonation Products of Hydrazine for Garcia- Large NH3 Covolume

Pressure = 5.0000000E-01 Volume = 5.6719090E-01 Temperature = l.1385820E+03 Shock Velocity = 1.0767470E+00 Particle Velocity = 4.5930810000E-01

specie	No of Moles
n2	1.0000040E+00
h2	2.0000110E+00
nh3	1.0000000E-08
h	1.0000000E-08

Pressure = 3.5000000E-01 Volume = 6.1738180E-01 Temperature = 7.6995310E+02 Shock Velocity = 9.5976260E-01 Particle Velocity = 3.6070470000E-01

Specie	No of Moles
n2	1.0000040E+00
h2	2.0000130E+00
nh3	1.0000000E-08
h	1.0000000E-08

Pressure = 2.0000000E-01 Volume = 7.0006750E-01 Temperature = 4.7937030E+02 Shock Velocity = 8.2276270E-01 Particle Velocity = 2.4043740000E-01

Specie	No of Moles
n2	1.0000040E+00
h2	2.0000130E+00
nh3	1.0000000E-08
h	1.0000000E-08

A BKW Isentrope thru BKW CJ Pressure for Hydrazine for Garcia- Large NH3 Covolume

ln(P)= -2.7180350E+00 -3.6537590E+00lnV -6.0775230E-0llnV*2
8.7331600E-0llnV*3 -4.5526350E-0llnV*4

ln(T)= 6.1689300E+00 -l.5809880E+00lnV -9.8901980E-0llnV*2
8.3671260E-0llnV*3 -6.9144960E-0llnV*4

ln(E)= -1.3238010E+00 4.8534600E-0llnP 4.5983S00E-02lnP*2
7.3650140E-03lnP*3 -1. 1714560E-03lnP*4

The constant added to energies was 1.0000000E-01

Pressure (mb)	**Volume (c/g)**	**Temperature(k)**	**Energy + c**	**Gamma**	**Part Vel**
4.000000E-01	5.984694E-01	8.837187E+02	1.781302E-01	3.473855E+00	3.952975E-01
3.800000E-01	6.073924E-01	8.732439E+02	1.747069E-01	3.473307E+00	4.086729E-01
3.610000E-01	6.164239E-01	8.618810E+02	1.713657E-01	3.472715E+00	4.217697E-01
3.429500E-01	6.255950E-0l	8.503550E+02	1.681394E-01	3.472113E+00	4.346358E-01
3.258025E-01	6.349089E-01	8.387241E+02	1.650265E-01	3.471535E+00	4.472764E-01
3.095123E-01	6.443667E-01	8.270055E+02	1.620235E-01	3.471018E+00	4.596942E-01
2.940367E-01	6.539695E-01	8.152119E+02	1.591268E-01	3.470596E+00	4.718916E-01
2.793349E-01	6.637183E-01	8.033556E+02	1.563332E-01	3.470305E+00	4.838709E-01
2.653681E-01	6.736143E-01	7.914485E+02	1.536391E-01	3.470181E+00	4.956350E-01
2.520997E-01	6.836582E-01	7.795016E+02	1.510415E-01	3.470259E+00	5.071865E-01
2.394947E-01	6.938510E-01	7.675248E+02	1.485371E-01	3.470575E+00	5.185281E-01
2.2752OOE-01	7.041937E-01	7.555281E+02	1.461229E-01	3.471163E+00	5.296627E-01
2.161440E-01	7.146870E-01	7.435204E+02	1.437960E-01	3.472060E+00	5.405933E-01
2.053368E-01	7.253316E-01	7.315102E+02	1.415535E-01	3.473299E+00	5.513223E-01

1.950699E-01	7.361284E-01	7.195061E+02	1.393928E-01	3.474915E+00	5.618531E-01
1.853164E-01	7.470779E-01	7.075150E+02	1.373110E-01	3.476943E+00	5.721883E-01
1.760506E-01	7.581806E-01	6.955446E+02	1.353056E-01	3.479416E+00	5.823308E-01
1.672481E-01	7.694368E-01	6.836008E+02	1.333741E-01	3.482369E+00	5.922835E-01
1.588857E-01	7.808473E-01	6.716909E+02	1.315140E-01	3.485833E+00	6.020494E-01
1.509414E-01	7.924120E-01	6.598201E+02	1.297230E-01	3.489841E+00	6.116313E-01
1.433943E-01	8.041312E-01	6.479944E+02	1.279989E-01	3.494426E+00	6.210318E-01
1.362246E-01	8.160048E-01	6.362188E+02	1.263393E-01	3.499617E+00	6.302537E-01
1.294134E-01	8.280329E-01	6.244984E+02	1.247422E-01	3.505447E+00	6.3930OOE-01
1.229427E-01	8.402152E-01	6.128380E+02	1.232056E-01	3.511944E+00	6.481732E-01
1.167956E-01	8.525513E-01	6.012417E+02	1.217272E-01	3.519138E+00	6.568760E-01
1.109558E-01	8.650409E-01	5.897138E+02	1.203054E-01	3.527056E+00	6.654111E-01
1.054080E-01	8.776831E-01	5.782582E+02	1.189381E-01	3.535726E+00	6.737808E-01
l.001376E-01	8.904773E-01	5.668786E+02	1.176235E-01	3.545174E+00	6.819878E-01
9.513070E-02	9.034225E-01	5.555784E+02	1.163599E-01	3.555424E+00	6.900346E-01
9.037416E-02	9.165174E-01	5.443610E+02	1.151457E-01	3.566502E+00	6.979234E-01
8.585545E-02	9.297607E-01	5.332294E+02	1.139790E-01	3.578429E+00	7.056565E-01
8.156268E-02	9.431508E-01	5.221863E+02	1.128584E-01	3.591227E+00	7.132362E-01
7.748455E-02	9.566861E-01	5.112347E+02	1.117823E-01	3.604916E+00	7.206648E-01
7.361032E-02	9.703645E-01	5.003771E+02	1.107491E-01	3.619514E+00	7.279444E-01
6.992980E-02	9.841837E-01	4.896159E+02	1.097575E-01	3.635039E+00	7.350769E-01
6.643331E-02	9.981413E-01	4.789534E+02	1.088061E-01	3.651507E+00	7.420644E-01
6.311164E-02	1.012235E+00	4.683918E+02	1.078934E-01	3.668931E+00	7.489088E-01
5.995606E-02	1.026461E+00	4.579332E+02	1.070182E-01	3.687324E+00	7.556121E-01
5.695825E-02	1.040816E+00	4.475794E+02	1.061792E-01	3.706695E+00	7.621759E-01
5.411034E-02	1.055297E+00	4.373322E+02	1.053752E-01	3.727054E+00	7.686020E-01
5.140482E-02	1.069900E+00	4.271935E+02	1.046049E-01	3.748407E+00	7.748922E-01
4.883458E-02	1.084621E+00	4.171650E+02	1.038672E-01	3.770759E+00	7.810479E-01
4.639285E-02	1.099455E+00	4.072479E+02	1.031610E-01	3.794111E+00	7.870709E-01
4.407321E-02	1.114397E+00	3.974441E+02	1.024852E-01	3.818465E+00	7.929627E-01
4.186955E-02	1.129442E+00	3.877548E+02	1.018388E-01	3.843819E+00	7.987246E-01
3.977607E-02	1.144585E+00	3.781812E+02	1.012207E-01	3.870167E+00	8.043580E-01
3.778727E-02	1.159820E+00	3.687248E+02	1.006300E-01	3.897504E+00	8.098643E-01
3.589790E-02	1.175140E+00	3.593865E+02	1.000657E-01	3.925819E+00	8.152449E-01
3.410301E-02	1.190538E+00	3.501678E+02	9.952678E-02	3.955102E+00	8.205010E-01
3.239786E-02	1.206008E+00	3.410694E+02	9.901247E-02	3.985337E+00	8.256336E-01
3.077796E-02	1.221541E+00	3.320927E+02	9.852186E-02	4.016508E+00	8.306444E-01
2.923906E-02	1.237130E+00	3.232383E+02	9.805410E-02	4.048594E+00	8.355341E-01
2.777711E-02	1.252767E+00	3.145072E+02	9.760838E-02	4.081573E+00	8.403040E-01
2.638825E-02	1.268442E+00	3.059005E+02	9.718390E-02	4.115419E+00	8.449551E-01
2.506884E-02	1.284l46E+00	2.974190E+02	9.677989E-02	4.150105E+00	8.494887E-01
4.200000E-01	5.901750E-01	8.950391E+02	1.815796E-01	3.474298E+00	0.000000E+00
4.410000E-01	5.819736E-0l	9.054424E+02	1.851060E-01	3.474640E+00	0.000000E+00
4.630499E-01	5.738980E-01	9.157203E+02	1.887549E-01	3.474850E+00	0.000000E+00
4.862024E-01	5.659454E-01	9.258l23E+02	1.925276E-01	3.474899E+00	0.000000E+00

FIGURE 6

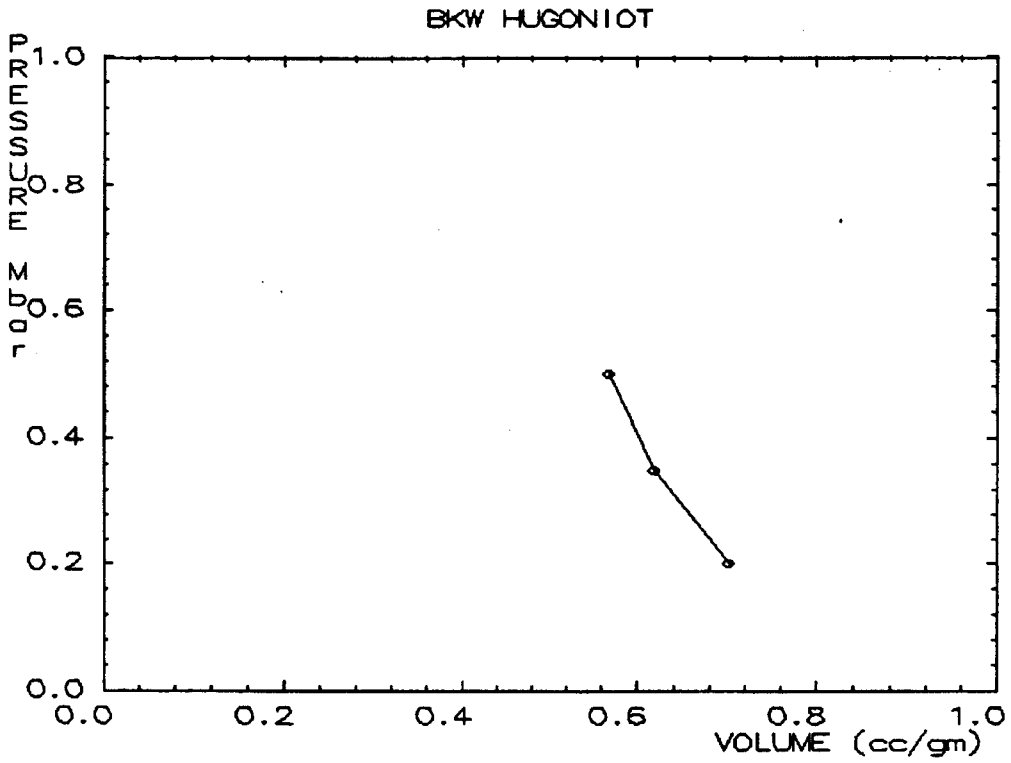
BKW HUGONIOT
PRESSURE Mbar
1.0
0.8
0.6
0.4
0.2
0.0
0.0
0.2
0.4
0.6
0.8
1.0
VOLUME (cc/gm)

FIGURE 7

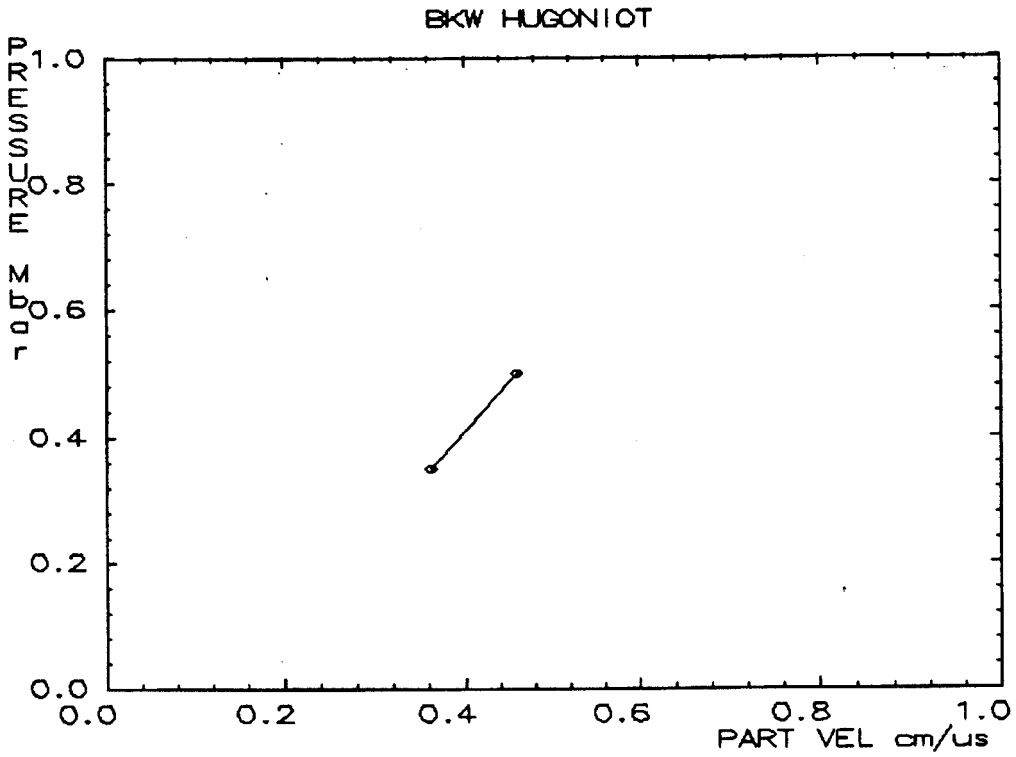
BKW HUGONIOT
PRESSURE Mbar
1.0
0.8
0.6
0.4
0.2
0.0
0.0
0.2
0.4
0.6
0.8
1.0
PART VEL cm/us

FIGURE 8

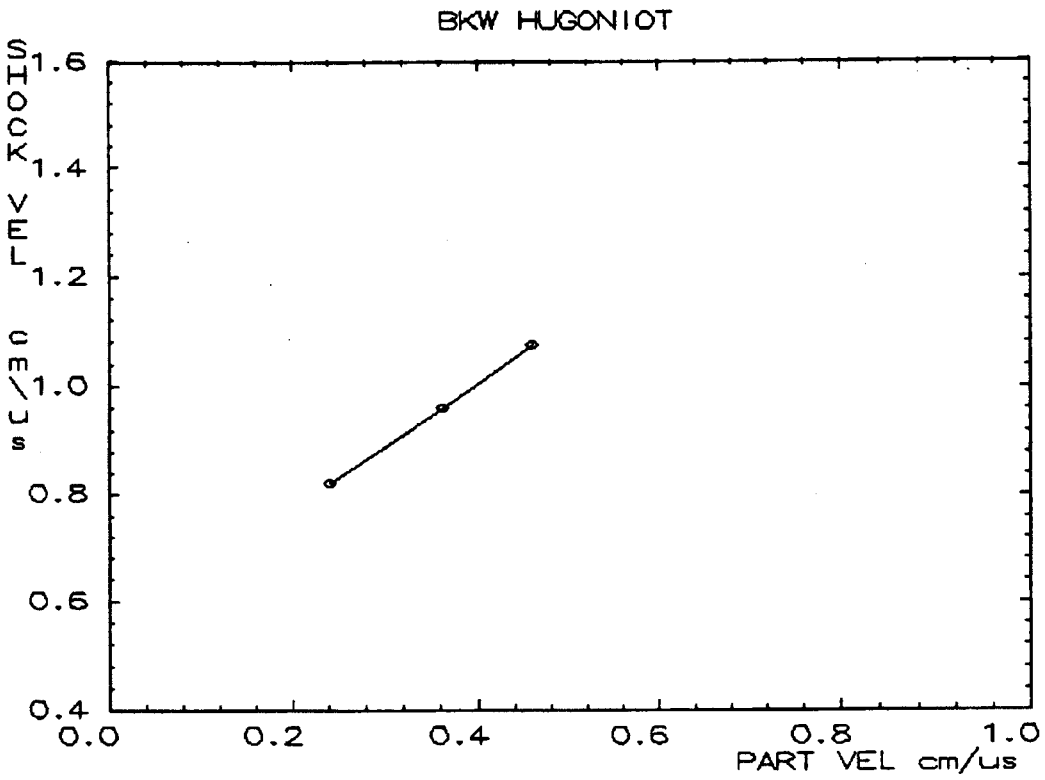
BKW HUGONIOT
SHOCK VEL cm/us
1.6
1.4
1.2
1.0
0.8
0.6
0.4
0.0
0.2
0.4
0.6
0.8
1.0
PART VEL cm/us

APPENDIX C
Thermal Stability Experiments

DETERMINATION OF HYDRAZINE DECOMPOSITION PARAMETERS

Jimmie Oxley; James Smith; Hongtu Feng; Evan Rogers; Nancy Gilson

New Mexico Institute of Mining and Technology
October 23, 1993

Accurate activation energy and pre-exponential factor values are essential for the SIN and TDL code calculations on hydrazine detonability. In this work we have determined these parameters over as wide a temperature range as possible.

Experimental Techniques

Hydrazine was transferred from the storage cylinder provided by Lockheed into a 5 mL septum cap vial inside a nitrogen-flushed glove bag. Inside the inert-atmosphere bag, hydrazine liquid was allowed to slowly fill the vial which was then capped with a screw-top septum prior to removal from the glove bag.

Outside the glove bag, hydrazine was quantitatively transferred (5 uL) from the nitrogen-filled vial into melting-point capillary tubes (1.8-mm o.d. by 6-cm long) using a 10 uL syringe. To avoid build-up of negative pressure in the septum vial, the syringe was filled with 5 uL of nitrogen gas which was injected into the septum vial, just prior to the removal of 5 uL of hydrazine. The melting-point capillary, into which the hydrazine was transferred, was flushed with argon until the hydrazine was added. At that point the inert gas f lush was switched to helium, and the melting-point capillary was f lame sealed. [The reason for the change in the inert gas fill was that although argon is a denser gas and provides a more reliable inert blanket, its retention time (GC) under the experimental conditions overlapped with that of nitrogen. Helium is, of course, invisible to in gas chromatography (GC) since it is the carrier gas.]

The capillaries of hydrazine were heated isothermally in a molten metal (Wood's metal) bath. At specific times samples were removed, and the progress of the decomposition was monitored by quantifying the evolved nitrogen gas up to that time. A Varian 3600 gas chromatograph (GC) equipped with a Haysep DB column, a thermal conductivity detector (TCD) , and helium carrier gas (20 mL/min.) was used. only two decomposition gases were observed: N2 with retention time about 7 minutes and NH, retention about 14 minutes. When quantification of decomposition of gases was desired, peak areas of each gas were compared against calibration curves for nitrogen and ammonia standards.

When the extent of decomposition was being assessed, the peak area of the nitrogen evolved after a given time of isothermal heating was ratioed against the peak area of nitrogen evolved

after complete decomposition. In this manner fraction reacted was determined. Plotting the logarithm of fraction remaining versus heating time produced a straight line, indicative of a first-order decomposition. The slope of that line was evaluated as the rate constant at that specific temperature.

Results and Discussion

Rate constants for hydrazine decomposition were found over a 130^0C temperature range using isothermal methods. Rate constants determined and the goodness of the linear-regression fit are shown in Table I. (Individual first-order plots are provided in the Appendix.) Using the rate constants obtained at ten temperatures, an Arrhenius plot was constructed (Fig. 1) and activation energy and frequency factor were calculated over the entire temperature range (26.8 kcal/mol and 6.51×10^6 sec^{-1}) and over the lower four temperatures (35.0 kcal/mol and 3.61×10^{10} sec^{-1} where there appeared to be a slight change in slope. Comparison to previously reported data is shown in Table II.[1,2]

Initial plans to quickly examine hydrazine thermal stability by scanning differential scanning calorimetry (DSC) were abandoned after several attempts produced irreproducible results. Decomposition kinetics obtained by scanning DSC analysis are considered inferior to those obtained by isothermal methods, but the DSC method is usually quicker. In the case of hydrazine, kinetics obtained by DSC have been published (Table II). However, after numerous attempts, it was deemed a waste of time and money to pursue this method. Because of the volatility of hydrazine, the hydrazine sample must be in a pressure tight container. The pressure-tight vessels we commonly use are flame sealed microcapillaries (about l cm long) . For hydrazine, this meant the flame used to seal the capillaries came quite close to the sample and evidently produced varying amounts of decomposition in various samples.

The decomposition gases were examined at both the high (275^0C) and low(190 C)endof the temperature range examined. The relative ratio of nitrogen to ammonia produced at these temperatures did not significantly vary (Fig. 2). Ther%fore, desgite the slight kink in the Arrhenius plot between 250 and 240 C, we cannot claim that the mechanism changes over this temperature range.

$$3\ N_2H_4 \rightarrow 1\ N_2 + 4\ NH_3$$

References

1. Welich, R.C.; Davis, D. D. Therinochimica Acta, 1990, 171, 1-13.

2. Bishop, C.V.; Miller, E.L.; Benz, F.J. "Liquid Propellant Thermal Hazards Estimation Using Differential Scanning Calorimetry" JANNAF Safety and Environmental Protection Subcommittee Meeting, 1983.

3. Anworthy, A.E.; Sullivan, J.M.; Cohy, S.; Wely, E. "Research on Hydrazine Decomposition" Final Report AFRPL-TR-69-146 Rocketdyne, Canoga Park, CA, July 1969.

Table I
Rate Constants of N_2H_4 Decomposition

°C	k sec^{-1}	R^2
184	6.55E-07	0.97
200	2.54E-06	0.95
220	1.26E-05	0.96
240	4.25E-05	0.97
250	4.49E-05	0.98
260	7.06E-05	0.95
270	1.09E-04	0.98
290	2.69E-04	0.92
300	3.21E-04	0.96
314	5.58E-04	0.98

Tab1e I Rate Constants of N_2H_4 Decomposition

Table II
Arrhenius Parameters of N_2H_4 Decomposition

	Isothermal (this work)		DSC[2]	ARC[1]	Isotherma
Ea (kcal/mol)	26.8	35.0	17	23.4	20.5
A (sec^{-1})	6.51E+06	3.61E+10	3.5E+06		
R^2 Fit	0.98	1.0			
Temp Range (°C)	280-184	184-240	317-202		

Table II Arrhenius Parameters of N_2H_4 Decomposition

Figure 9 Hydrazine Arrhenius Plot
(Appendix C, Fig. 1)

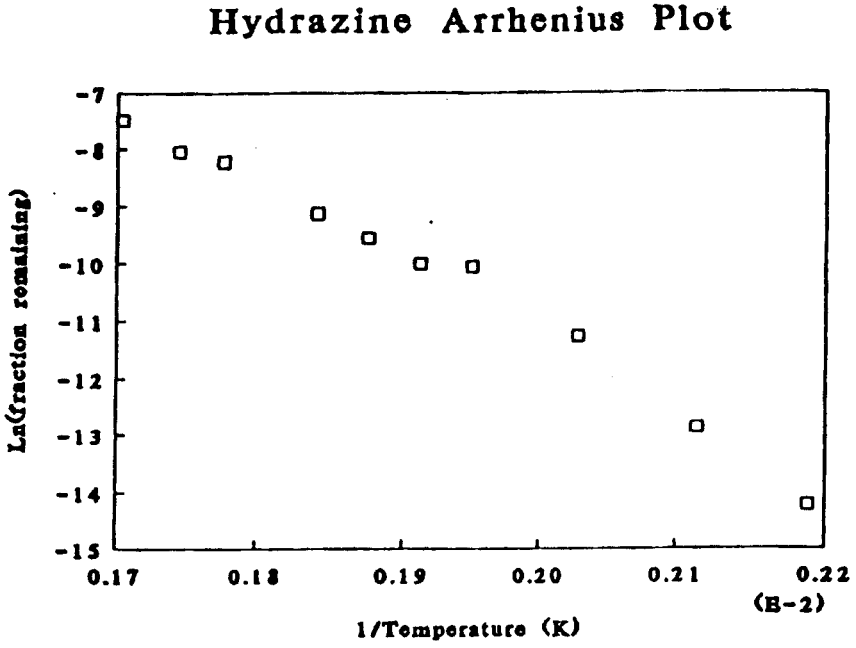

°C	k sec^{-1}	R^2
184	6.55e-07	0.97
200	2.54e-06	0.95
220	1.26e-05	0.96
240	4.25e-05	0.97
250	4.49e-05	0.98
260	7.06e-05	0.95
270	1.09e-04	0.98
290	2.69e-04	0.92
300	3.21e-04	0.96
314	5.58e-04	0.98

Fig. 1

Figure 10
Gas evolved at 190°C and Gas evolved at 275°C

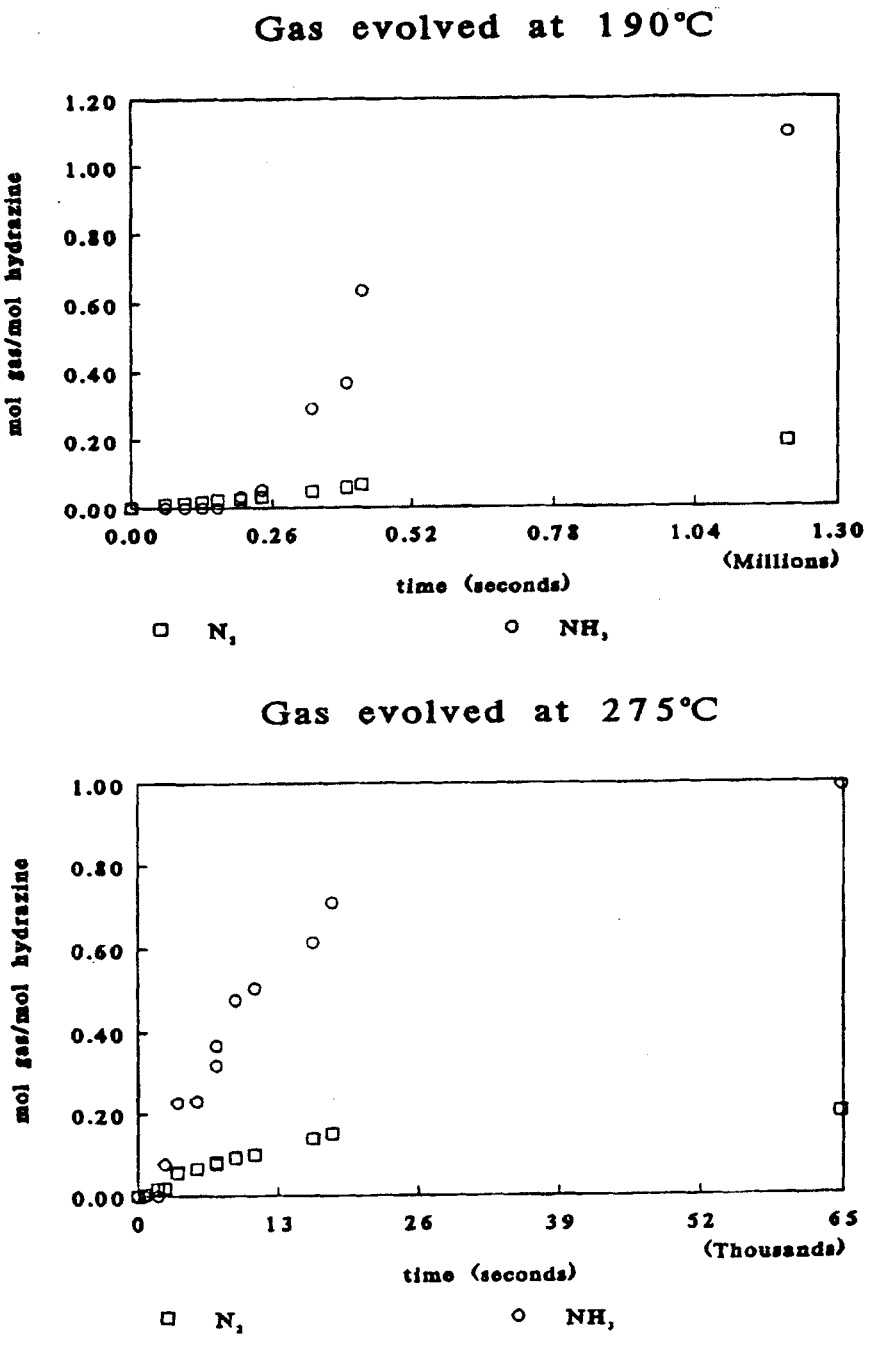

Fig. 2

(Appendix C, Fig. 2)
Figure 11
Hydrazine at 1 84^{0}C HPLC Data and Hydrazine at 200^{0}C HPLC Data

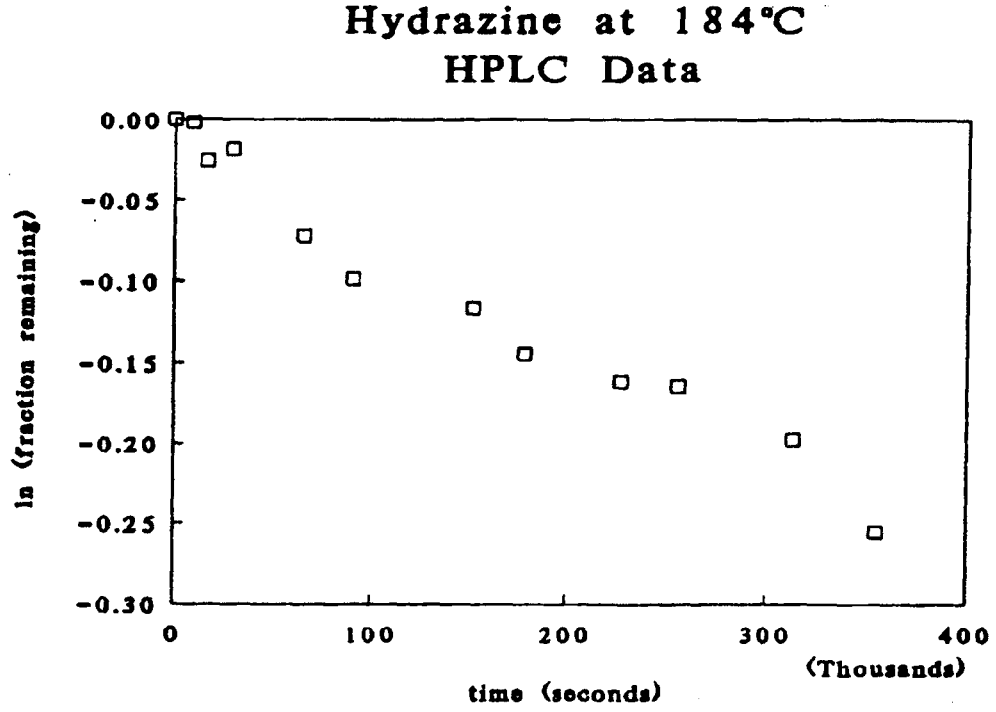

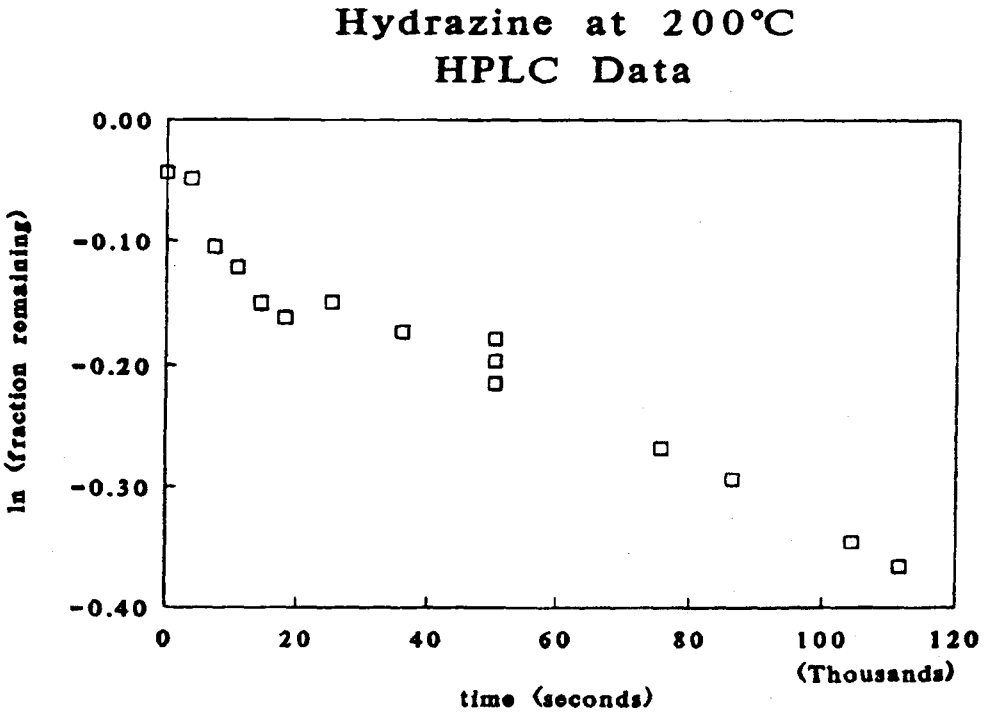

Figure 12
Hydrazine at 220^{0}C HPLC Data and Hydrazine at 240*C HPLC Data

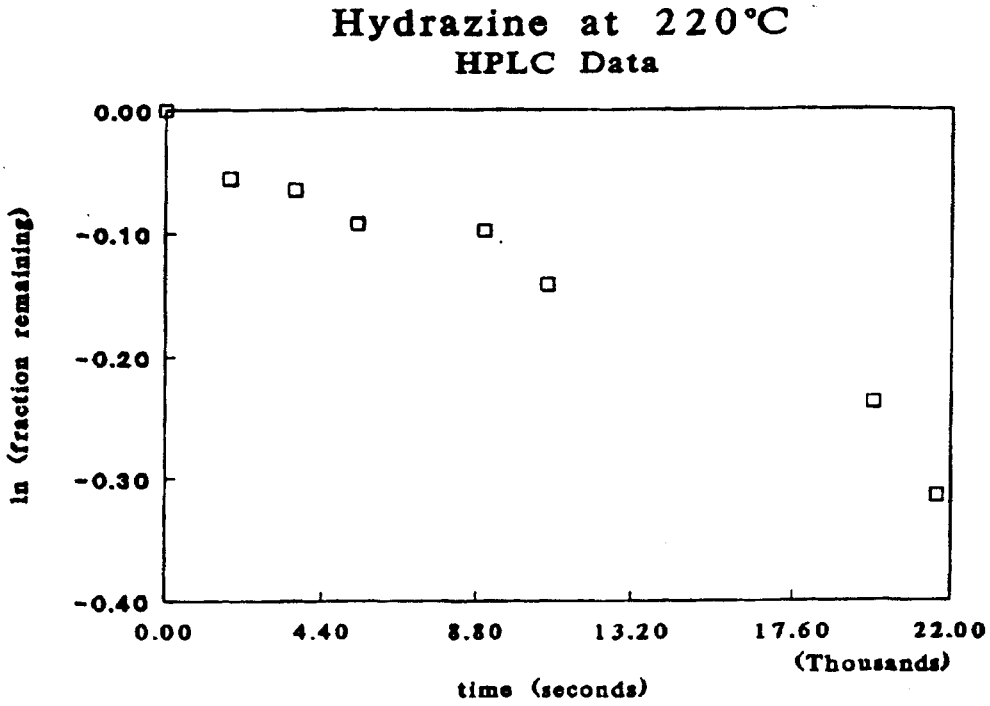

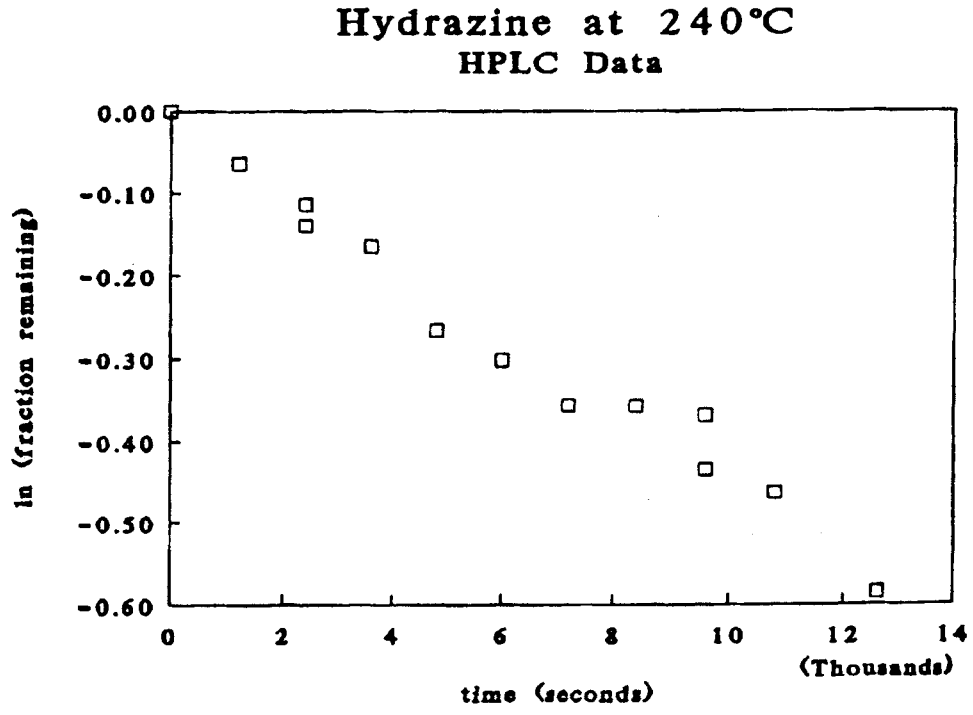

Figure 13
Hydrazine at 250^{0}C HPLC Data and Hydrazine at 260*C HPLC Data

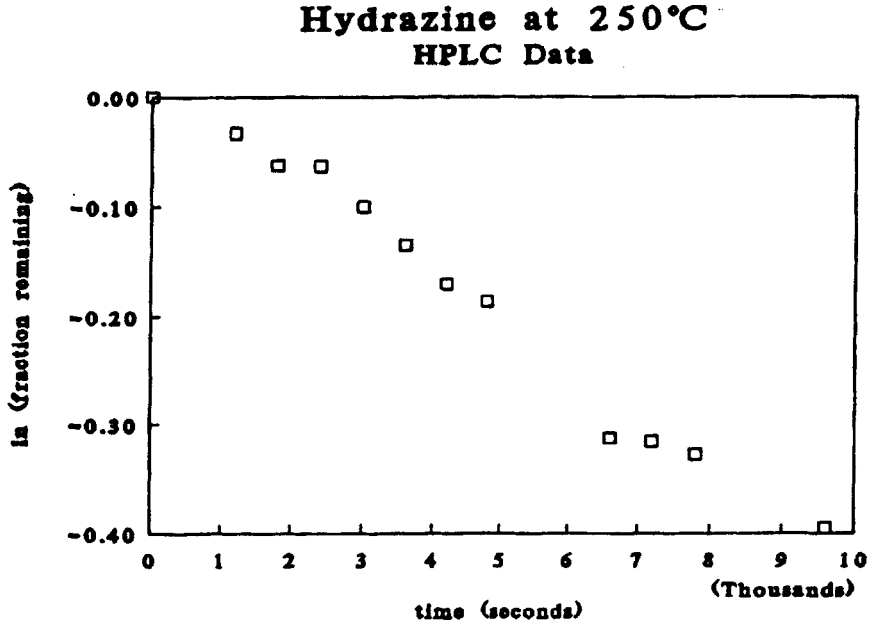

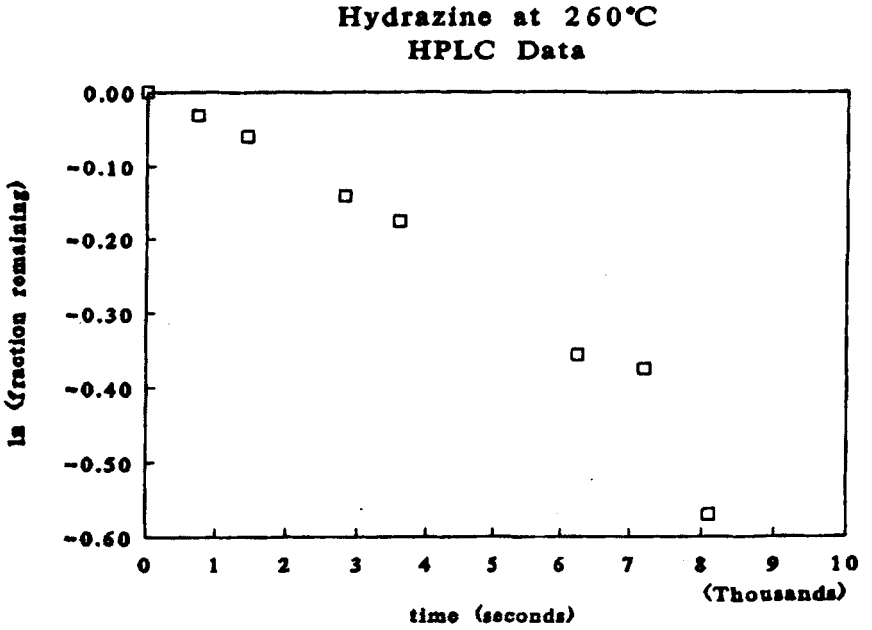

Figure 14
Hydrazine at 290^{0}C HPLC Data and Hydrazine at 300*C HPLC Data

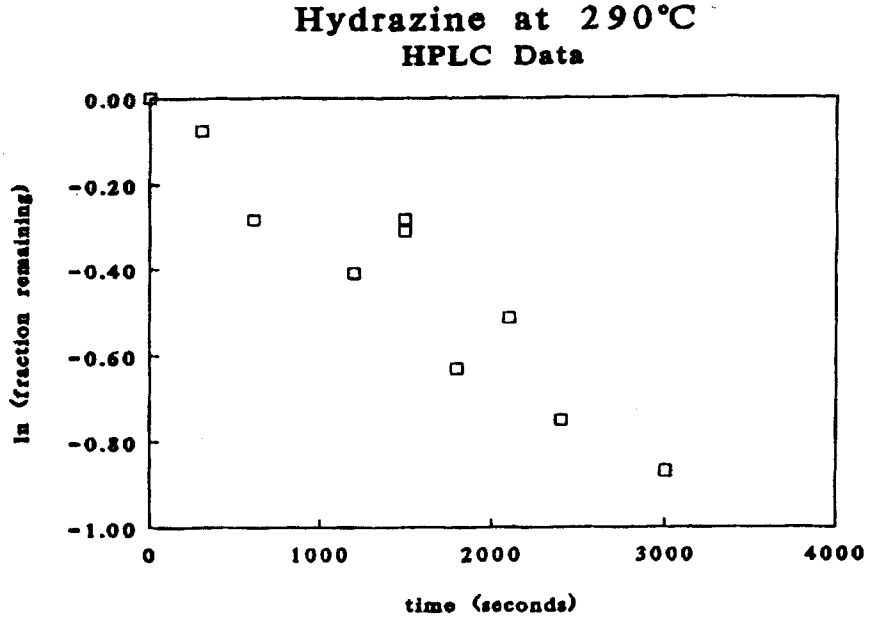

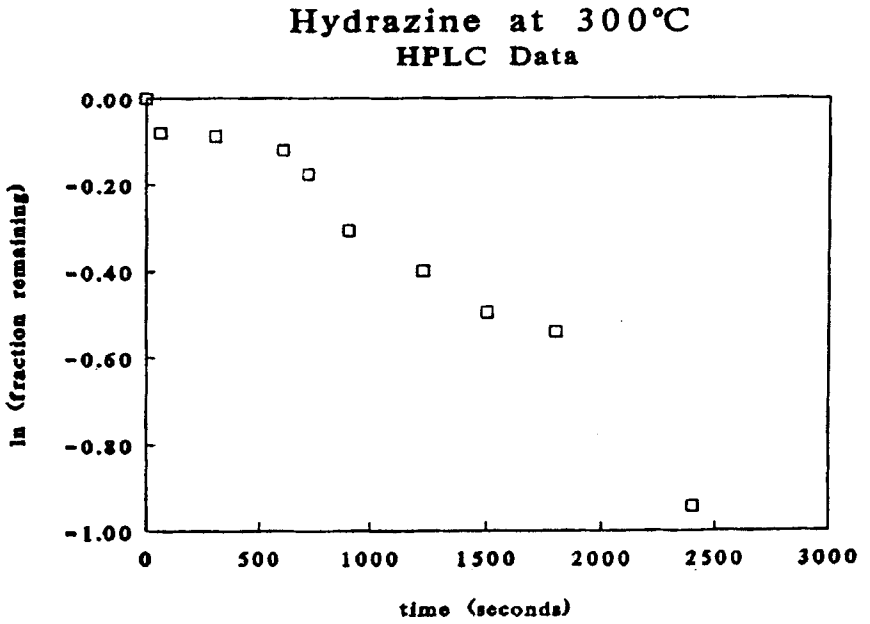

Figure 15
Hydrazine at 314^{0}C HPLC Data

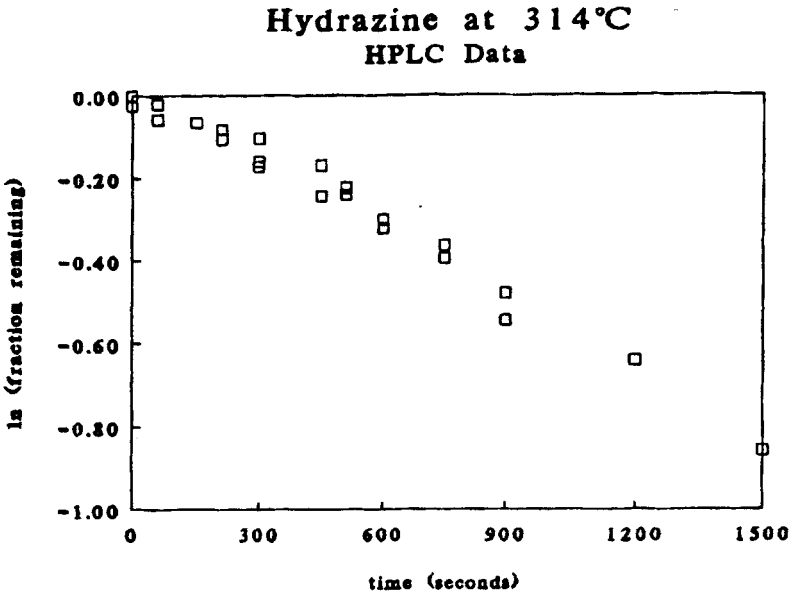

Figure 16
APPENDIX D
(Figure 1 of Appendix D)
Figure 1 Condensed Phase Detonation Study SIN calculation of the shock pressure into liquid hydrazine

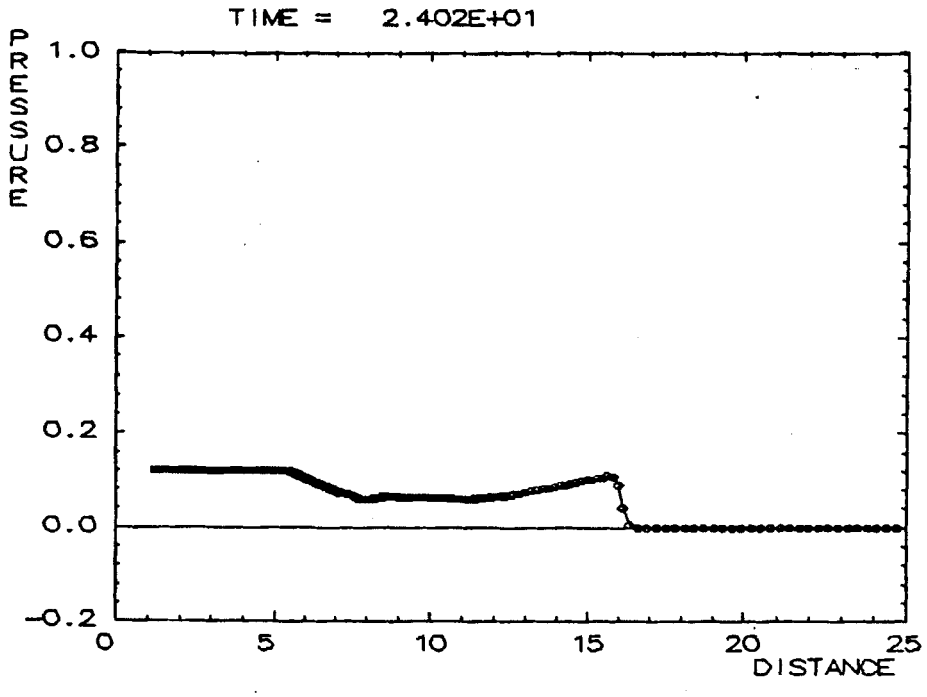

Figure 1
Condensed Phase Detonation Study
SIN calculation of the shock pressure into liquid hydrazine

Figure 17
(Figure 2 of Appendix D)
Figure 2 Condensed Phase Detonation Study No hydrazine reaction

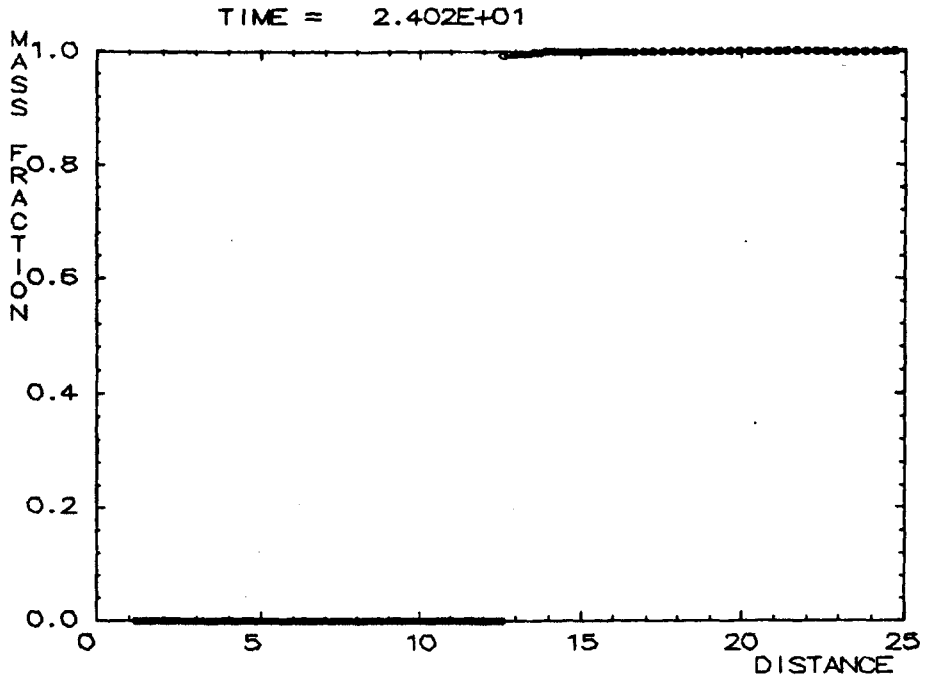

Figure 2
Condensed Phase Detonation Study
No hydrazine reaction

Figure 18
(Figure 3 of Appendix D)
Figure 3 Demonstration Hazardous Hypervelocity Test Zeus calculation of the shock pressure into the liquid hydrazine

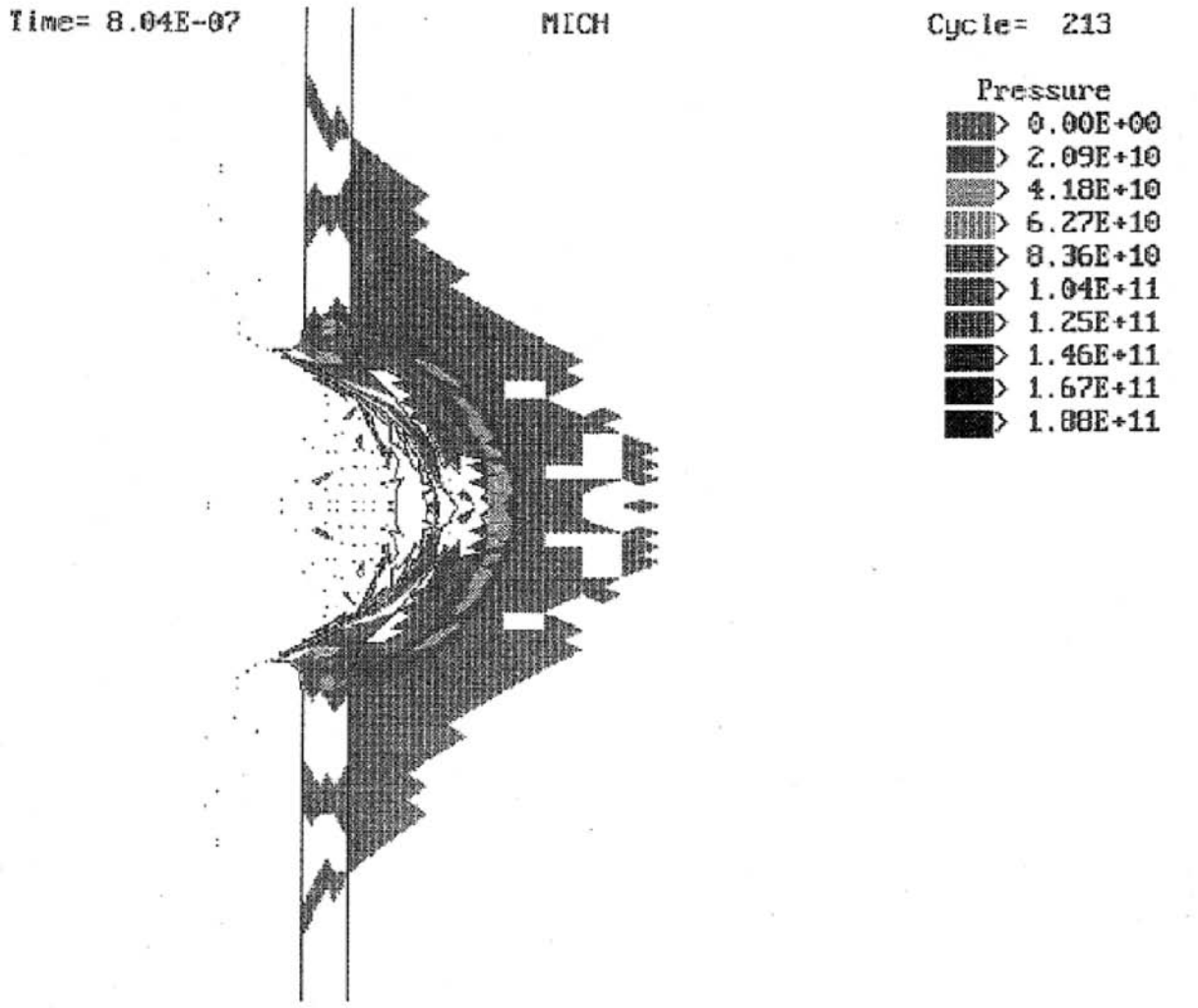

Figure 3
Demonstration of Hazardous Hypervelocity Test
Zeus calculation of the shock pressure into the liquid hydrazine

Figure 19
(Figure 4 of Appendix D)
Figure 4 Demonstration of Hazardous Hypervelocity Test TDL calculation of projectile impacting the cylindrical vessel for the. No hydrazine reaction.

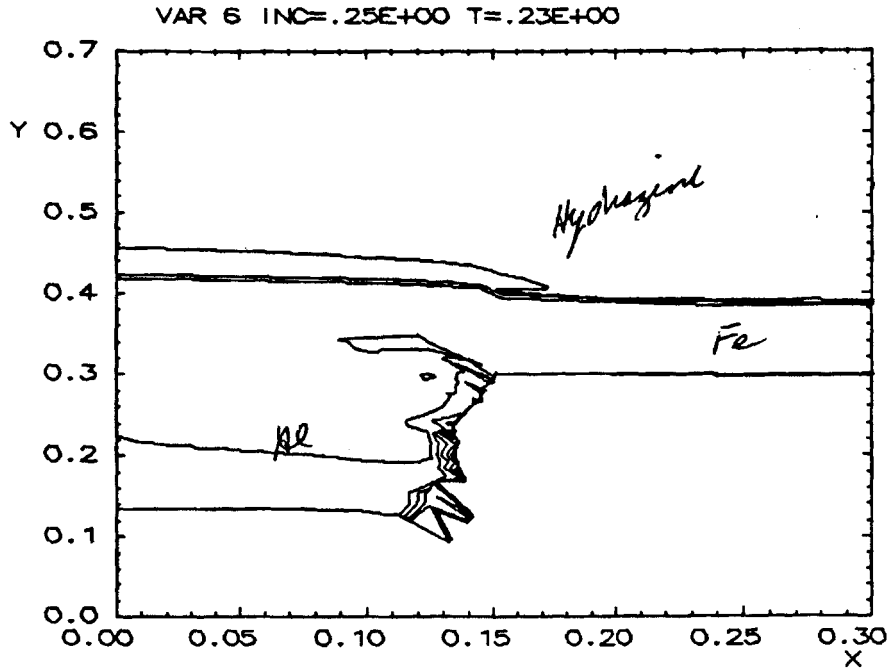

Figure 4
Demonstration of Hazardous Hypervelocity Test
TDL calculation of projectile impacting the cylindrical vessel for the. No hydrazine reaction.

Figure 20
(Figure 5 of Appendix D)
Figure 5 Demonstration of Hazardous Hypervelocity Test TDL calculation of the shock pressure into the hydrazine. No hydrazine reaction.

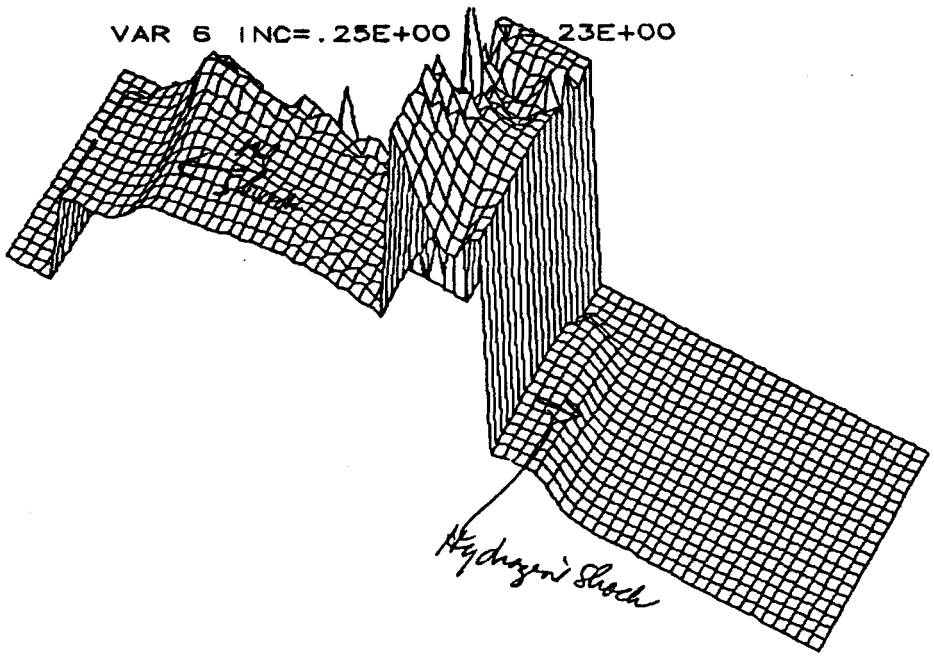

Figure 5
Demonstration of Hazardous Hypervelocity Test
TDL calculation of the shock pressure into the hydrazine. No hydrazine reaction.

Figure 6
Shock matching curves for the SAIC Test

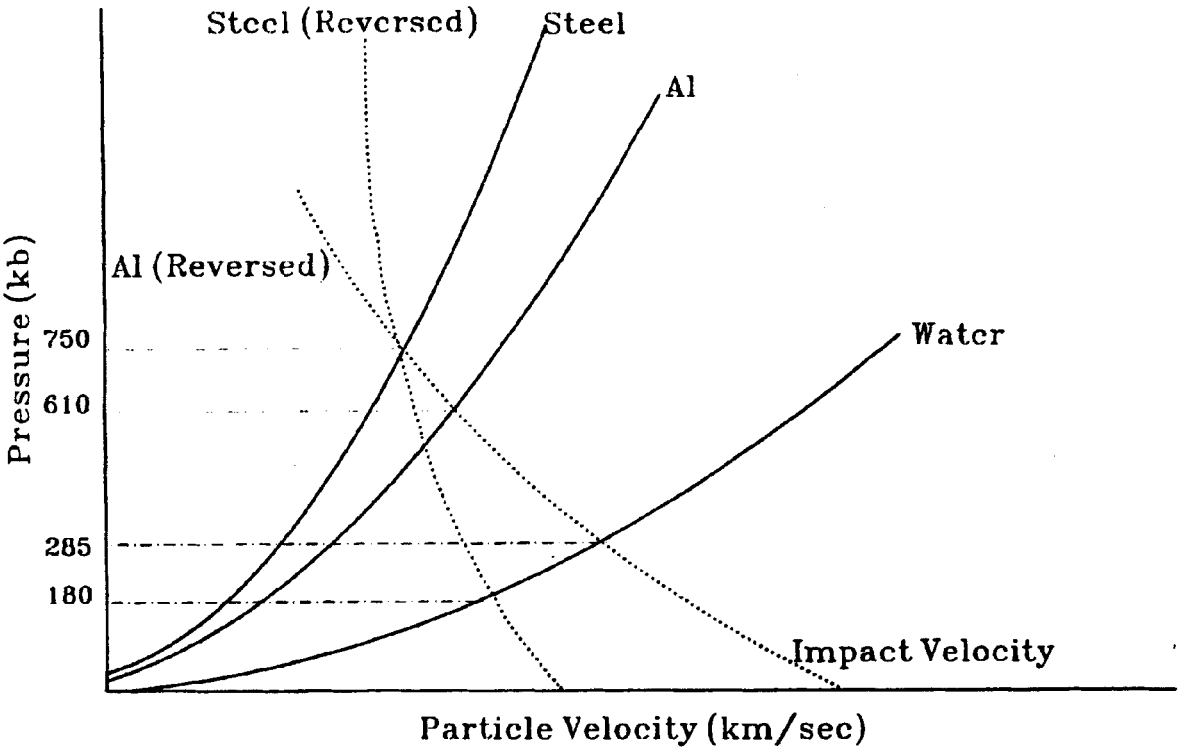

Figure 21
(Figure 6 of Appendix D)
Figure 6 Shock matching curves for the SAIC Test

Figure 7
Shock matching curves for the Condensed Phase Detonation Study

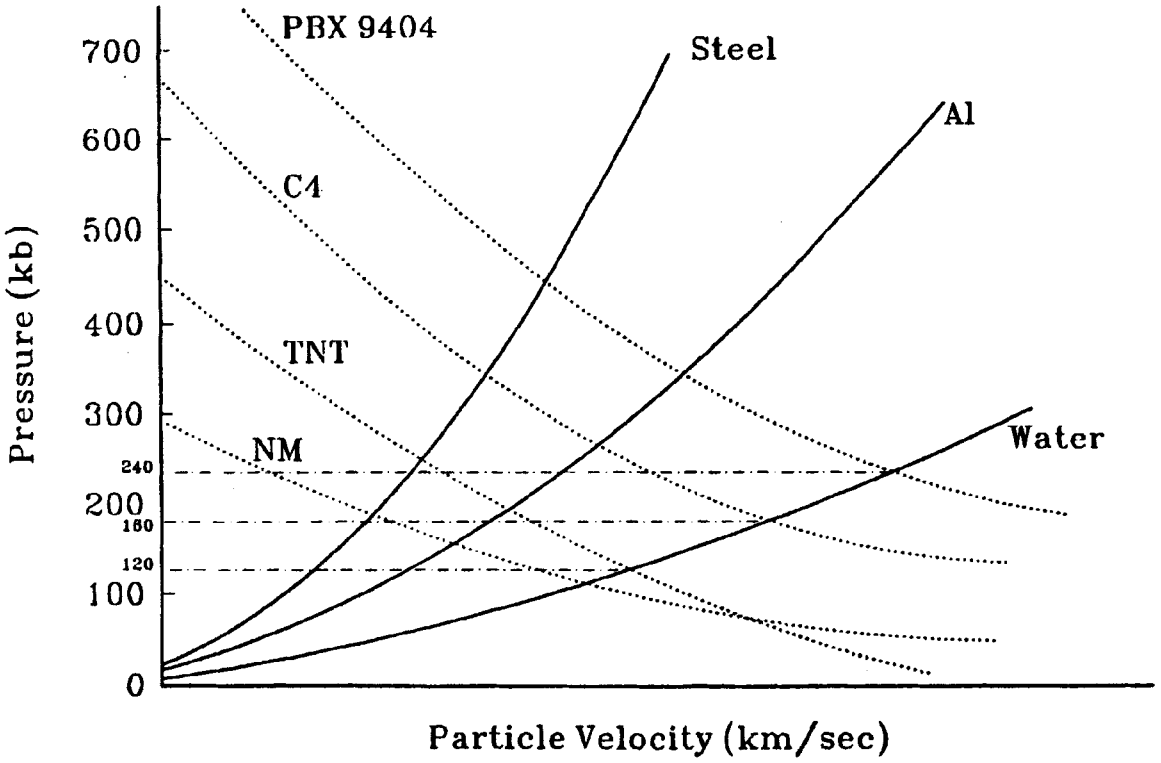

+Figure 22
(Figure 7 of Appendix D)
Figure 7 Shock matching curves for the Condensed Phase Detonation Study

Figure 23
(Figure 8 of Appendix D)
Figure 8 SAIC Test
SIN calculation of the shock pressure into the liquid hydrazine

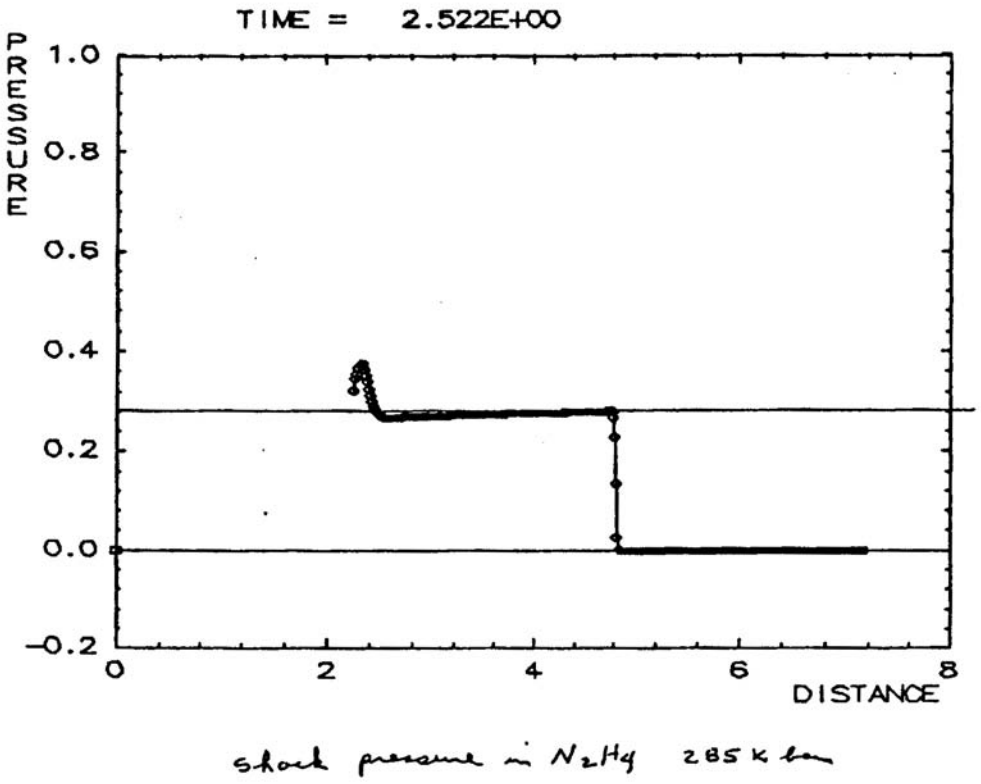

Figure 8
SAIC Test
SIN calculation of the shock pressure into the liquid hydrazine

Figure 24
(Figure 9 of Appendix D)
Figure 9 SAIC Test
Hydrazine decomposition

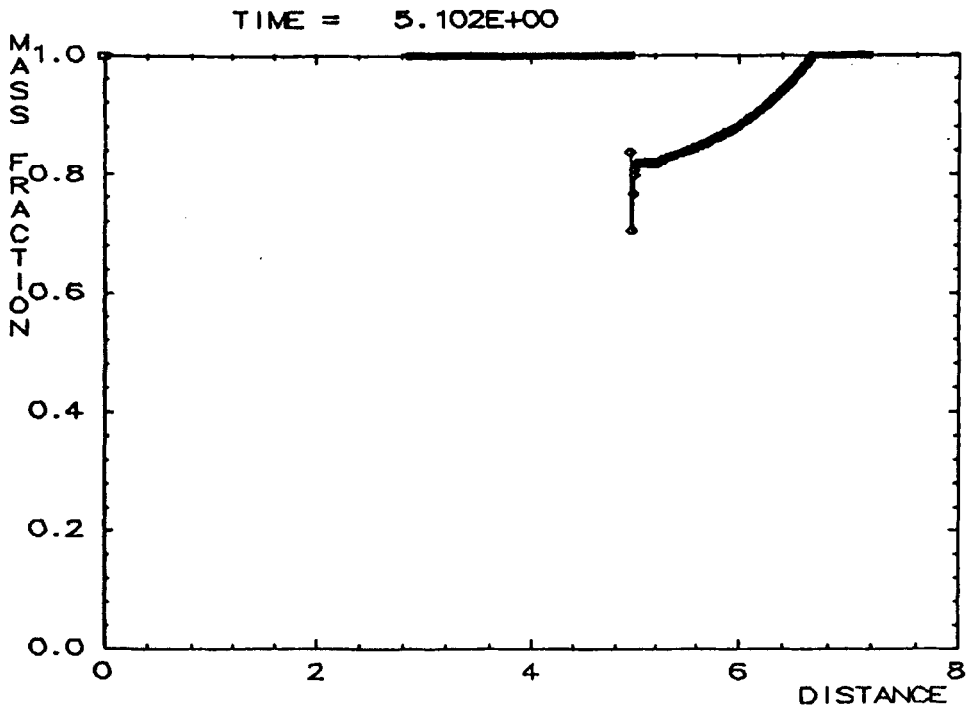

Figure 9
SAIC Test
Hydrazine decomposition

Figure 25
(Figure 10 of Appendix D)
Figure 10 SMC Test
Zeus calculation of the shock pressure into the liquid hydrazine

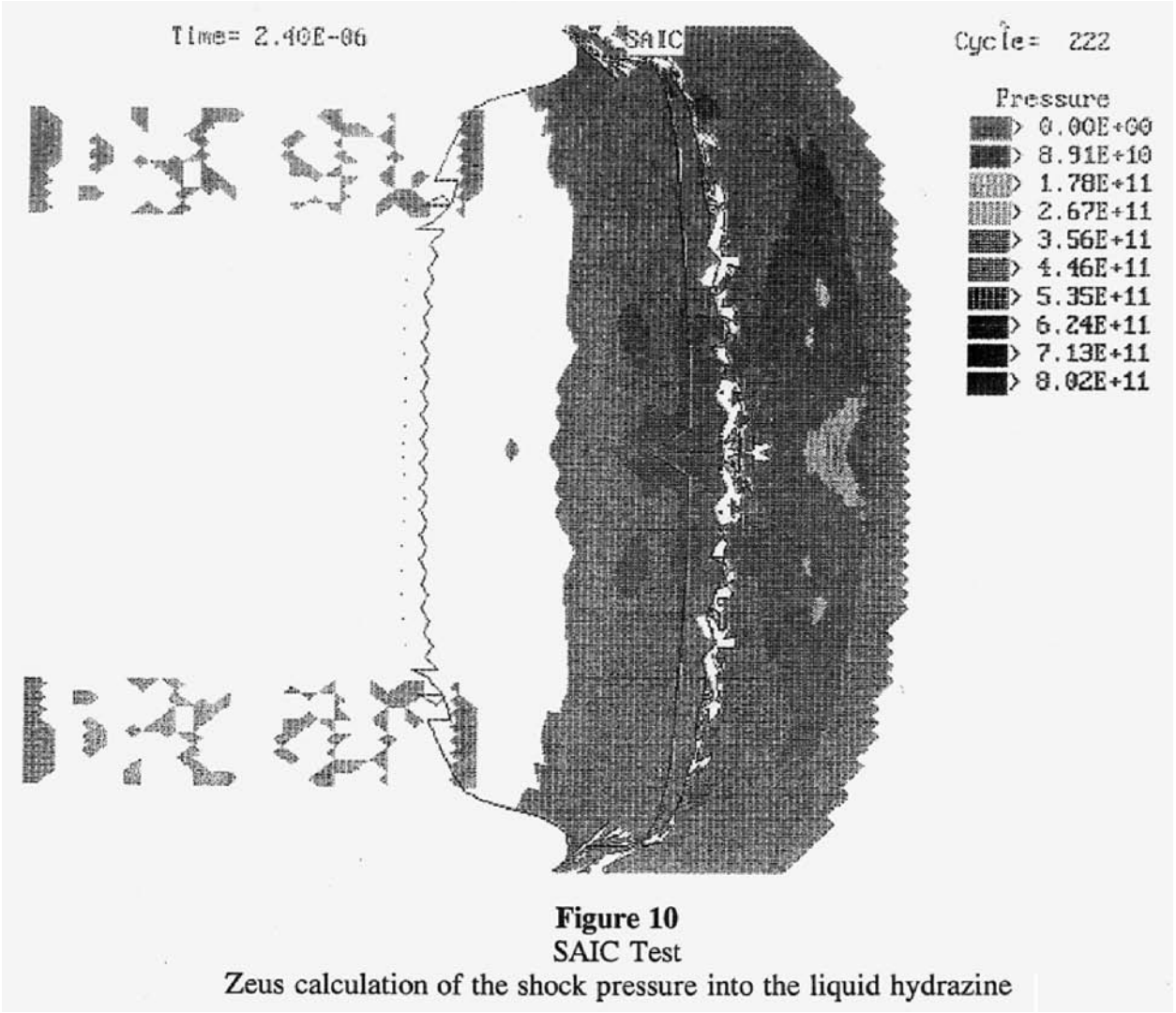

Figure 10
SAIC Test
Zeus calculation of the shock pressure into the liquid hydrazine

Figure 26
(Figure 11 of Appendix D)
Figure 11 Proposed Experiment
SIN calculation of the shock pressure generated into the liquid hydrazine

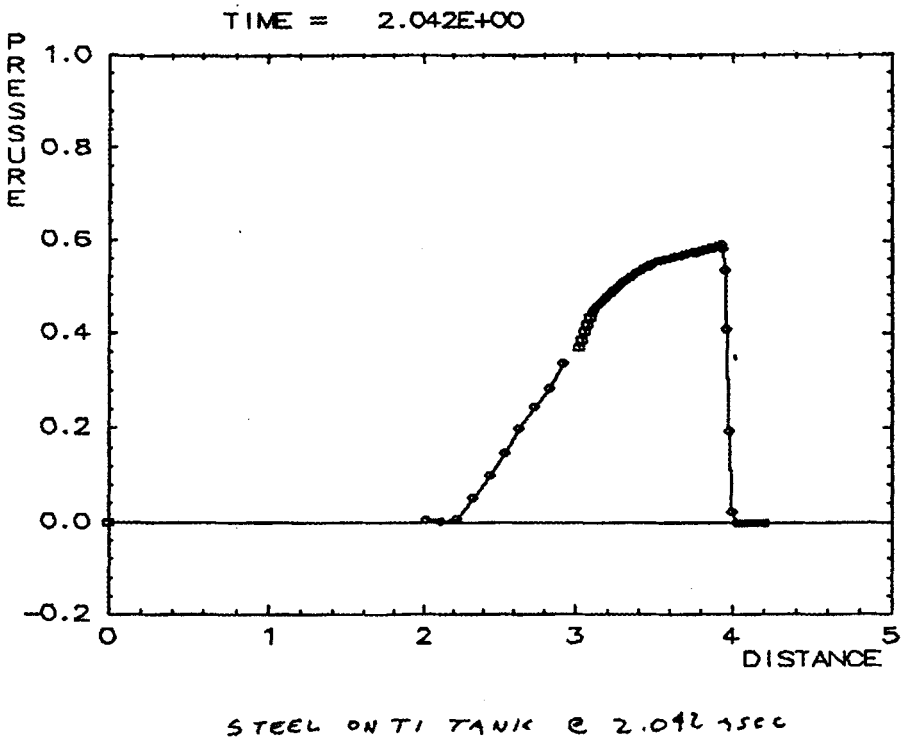

Figure 11
Proposed Experiment
SIN calculation of the shock pressure generated into the liquid hydrazine

Figure 27
(Figure 12 of Appendix D)
Figure 12 Proposed Experiment
SIN calculation of the amount of hydrazine decomposition

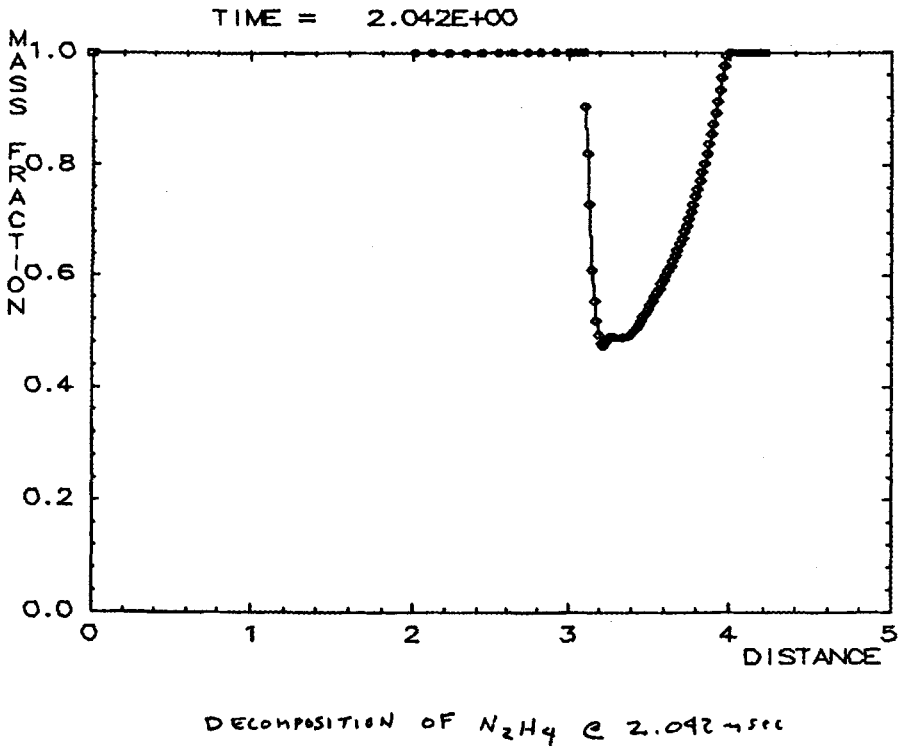

Figure 12
Proposed Experiment
SIN calculation of the amount of hydrazine decomposition

Figure 28
(Figure 13 of Appendix D)
Figure 13 Proposed Experiment
TDL calculation of the amount of hydrazine decomposition

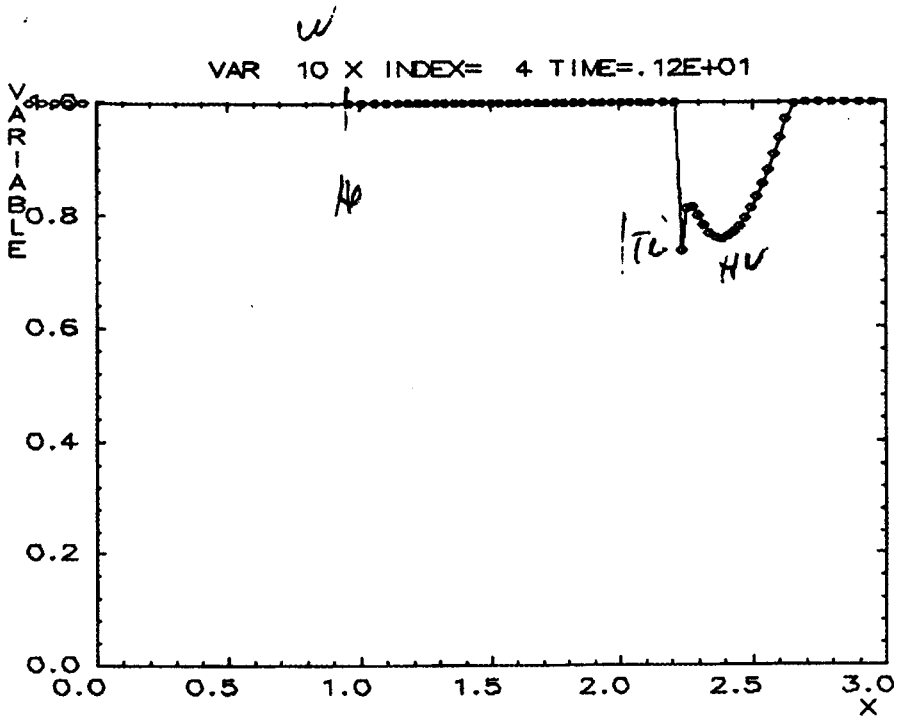

Figure 13
Proposed Experiment
TDL calculation of the amount of hydrazine decomposition

Figure 29
(Figure 14 of Appendix D)
Figure 14 Proposed Experiment
Zeus calculation of the shock pressure into the liquid hydrazine

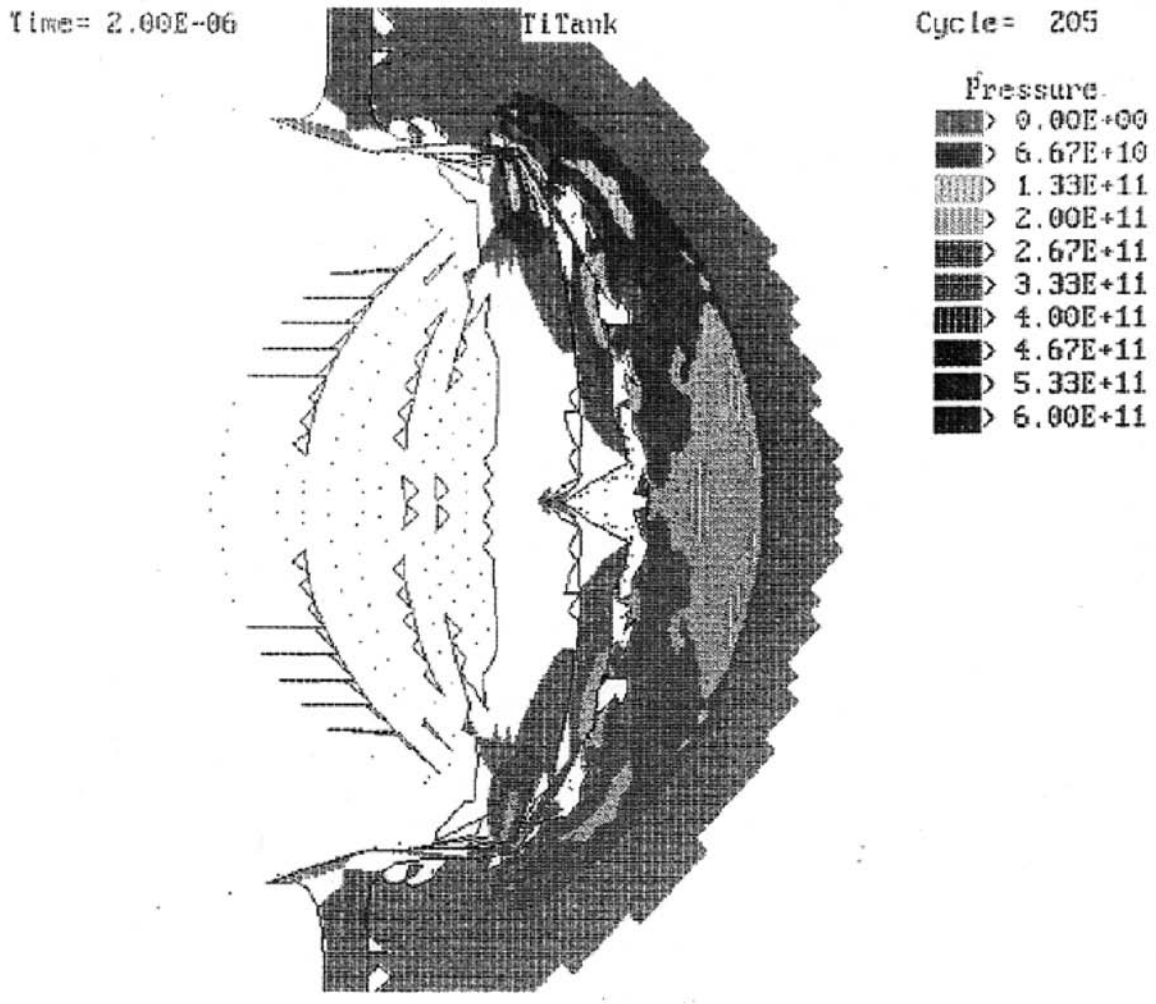

Figure 14
Proposed Experiment
Zeus calculation of the shock pressure into the liquid hydrazine

TABLE 1

REACTIVE ANALYSIS OF TESTS

TEST	TEST CONDITION	SIN (1-D)			ZEUS		POWER DENSITY (KB ^ 2-SEC)
		PRESSURE (KBAR)	DURATION (MICROSEC)	MASS FRACTION	PRESSURE (KBAR)	DURATION (MICROSEC)	
WSTF #1	C4 on N2H4	150	0.7	.99	---	---	0.016
WSTF#2	1/8" AL impacting N2H4 @ 6KM/S	---	---	---	83 62.7	T0 0.8	~~0.924~~ 0.0024
SAIC	AL slug (2cm) impacting AL sphere filled w/ N2H4 @ 5KM/S	285	5	0.81	267 267 178 178	T0 1.5 1.8 2.4	0.137
TITANK	STL slug (1 CM) impacting TI tank filled w/ N2H4 @ 7.5KM/S	600	2.4	0.58	600 444 300 178	T0 1 1.5 2	0.398

Table III
(Table 1 of Appendix D)
Table 1 Reactive Analysis of Tests